Annals of Mathematics, **160** (2004), 27–68

The space of embedded minimal surfaces of fixed genus in a 3-manifold I; Estimates off the axis for disks

By Tobias H. Colding and William P. Minicozzi II*

0. Introduction

This paper is the first in a series where we describe the space of all embedded minimal surfaces of fixed genus in a fixed (but arbitrary) closed Riemannian 3-manifold. The key for understanding such surfaces is to understand the local structure in a ball and in particular the structure of an embedded minimal disk in a ball in $\mathbf{R}^3$ (with the flat metric). This study is undertaken here and completed in [CM6]. These local results are then applied in [CM7] where we describe the general structure of fixed genus surfaces in 3-manifolds.

There are two local models for embedded minimal disks (by an embedded disk, we mean a smooth injective map from the closed unit ball in $\mathbf{R}^2$ into $\mathbf{R}^3$). One model is the plane (or, more generally, a minimal graph), the other is a piece of a helicoid. In the first four papers of this series, we will show that every embedded minimal disk is either a graph of a function or is a double spiral staircase where each staircase is a multi-valued graph. This will be done by showing that if the curvature is large at some point (and hence the surface is not a graph), then it is a double spiral staircase. To prove that such a disk is a double spiral staircase, we will first prove that it is built out of N-valued graphs where N is a fixed number. This is initiated here and will be completed in the second paper. The third and fourth papers of this series will deal with how the multi-valued graphs fit together and, in particular, prove regularity of the set of points of large curvature – the axis of the double spiral staircase.

The reader may find it useful to also look at the survey [CM8] and the expository article [CM9] for an outline of our results, and their proofs, and how these results fit together. The article [CM9] is the best to start with.

*The first author was partially supported by NSF Grant DMS 9803253 and an Alfred P. Sloan Research Fellowship and the second author by NSF Grant DMS 9803144 and an Alfred P. Sloan Research Fellowship.

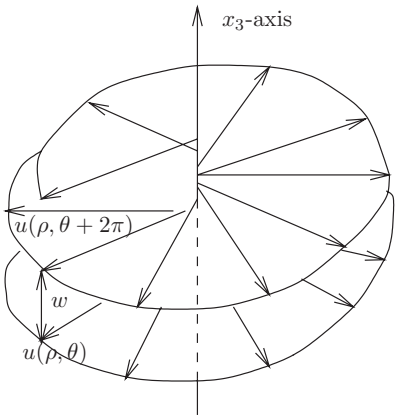

Figure 1: The separation of a multi-valued graph.

Our main theorem about embedded minimal disks is that every such disk can either be modelled by a minimal graph or by a piece of the helicoid depending on whether the curvature is small or not; see Theorem 0.2 below. This will be proven in [CM6] with the first steps taken here. The helicoid is the minimal surface in $\mathbf{R}^3$ parametrized by $(s\cos(t), s\sin(t), t)$ where $s, t \in \mathbf{R}$.

To be able to discuss the helicoid some more and in particular give a precise meaning to the fact that it is like a double spiral staircase, we will need the notion of a multi-valued graph; see Figure 1. Let D_r be the disk in the plane centered at the origin and of radius r and let $\mathcal{P}$ be the universal cover of the punctured plane $\mathbf{C} \setminus \{0\}$ with global polar coordinates (ρ, θ) so that $\rho > 0$ and $\theta \in \mathbf{R}$. An N-valued graph of a function u on the annulus $D_s \setminus D_r$ is a single valued graph over

$$\{(\rho, \theta) \,|\, r \leq \rho \leq s\,,\ |\theta| \leq N\,\pi\}\,. \tag{0.1}$$

The middle sheet Σ^M (an annulus with a slit as in [CM3]) is the portion over

$$\{(\rho, \theta) \in \mathcal{P} \,|\, r \leq \rho \leq s \text{ and } 0 \leq \theta \leq 2\,\pi\}\,.$$

The multi-valued graphs that we will consider will never close up; in fact they will all be embedded. Note that embedded means that the separation never vanishes. Here the separation (see Figure 1) is the function given by

$$w(\rho, \theta) = u(\rho, \theta + 2\pi) - u(\rho, \theta)\,.$$

If Σ is the helicoid (see Figure 2), then $\Sigma \setminus x_3 - \text{axis} = \Sigma_1 \cup \Sigma_2$, where Σ_1, Σ_2 are ∞-valued graphs. Also, Σ_1 is the graph of the function $u_1(\rho, \theta) = \theta$ and Σ_2 is the graph of the function $u_2(\rho, \theta) = \theta + \pi$. In either case the separation $w = 2\,\pi$. A multi-valued minimal graph is a multi-valued graph of a function u satisfying the minimal surface equation.

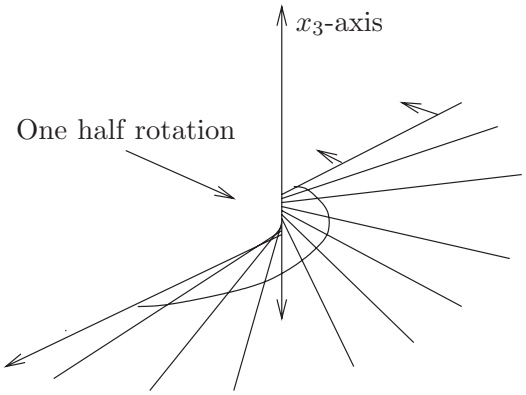

Figure 2: The helicoid is obtained by gluing together two ∞-valued graphs along a line. The two multi-valued graphs are given in polar coordinates by $u_1(\rho,\theta) = \theta$ and $u_2(\rho,\theta) = \theta + \pi$. In either case $w(\rho,\theta) = 2\,\pi$.

Here, we have normalized so that our embedded multi-valued graphs have positive separation. This can be achieved after possibly reflecting in a plane.

Let now $\Sigma_i \subset B_{2R}$ be a sequence of embedded minimal disks with $\partial\Sigma_i \subset \partial B_{2R}$. Clearly (after possibly going to a subsequence) either (1) or (2) occur:

(1) $\sup_{B_R \cap \Sigma_i} |A|^2 \leq C < \infty$ for some constant C.

(2) $\sup_{B_R \cap \Sigma_i} |A|^2 \to \infty$.

In (1) (by a standard argument) the intrinsic ball $\mathcal{B}_s(y_i)$ is a graph for all $y_i \in B_R \cap \Sigma_i$, where s depends only on C. Thus the main case is (2) which is the subject of the next theorem.

Using the notion of multi-valued graphs, we can now state our main theorem:

THEOREM 0.2 (Theorem 0.1 in [CM6] (see Figure 3)). *Let $\Sigma_i \subset B_{R_i} = B_{R_i}(0) \subset \mathbf{R}^3$ be a sequence of embedded minimal disks with $\partial\Sigma_i \subset \partial B_{R_i}$ where $R_i \to \infty$. If*

$$\sup_{B_1 \cap \Sigma_i} |A|^2 \to \infty\,,$$

then there exist a subsequence, Σ_j, and a Lipschitz curve $\mathcal{S} : \mathbf{R} \to \mathbf{R}^3$ such that after a rotation of $\mathbf{R}^3$:

(1) *$x_3(\mathcal{S}(t)) = t$. (That is, $\mathcal{S}$ is a graph over the x_3-axis.)*

(2) *Each Σ_j consists of exactly two multi-valued graphs away from $\mathcal{S}$ (which spiral together).*

(3) *For each $1 > \alpha > 0$, $\Sigma_j \setminus \mathcal{S}$ converges in the C^α-topology to the foliation, $\mathcal{F} = \{x_3 = t\}_t$, of $\mathbf{R}^3$.*

(4) $\sup_{B_r(\mathcal{S}(t))\cap\Sigma_j} |A|^2 \to \infty$ *for all* $r > 0$, $t \in \mathbf{R}$. (*The curvatures blow up along* $\mathcal{S}$.)

In (2), (3) that $\Sigma_j \setminus \mathcal{S}$ are multi-valued graphs and converge to $\mathcal{F}$ means that for each compact subset $K \subset \mathbf{R}^3 \setminus \mathcal{S}$ and j sufficiently large, $K \cap \Sigma_j$ consists of multi-valued graphs over (part of) $\{x_3 = 0\}$ and $K \cap \Sigma_j \to K \cap \mathcal{F}$ in the sense of graphs.

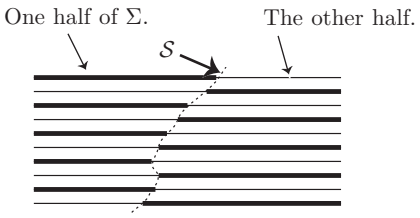

Figure 3: Theorem 0.2 — the singular set, $\mathcal{S}$, and the two multi-valued graphs.

Theorem 0.2 (like many of the other results discussed below) is modelled by the helicoid and its rescalings. Take a sequence $\Sigma_i = a_i \Sigma$ of rescaled helicoids where $a_i \to 0$. The curvatures of this sequence are blowing up along the vertical axis. The sequence converges (away from the vertical axis) to a foliation by flat parallel planes. The singular set $\mathcal{S}$ (the axis) then consists of removable singularities.

Before we proceed, let us briefly describe the strategy of the proof of Theorem 0.2.

The proof has the following three main steps; see Figure 4:

A. Fix an integer N (the "large" of the curvature in what follows will depend on N). If an embedded minimal disk Σ is not a graph (or equivalently if the curvature is large at some point), then it contains an N-valued minimal graph which initially is shown to exist on the scale of $1/\max|A|$. That is, the N-valued graph is initially shown to be defined on an annulus with both inner and outer radii inversely proportional to $\max|A|$.

B. Such a potentially small N-valued graph sitting inside Σ can then be seen to extend as an N-valued graph inside Σ almost all the way to the boundary. That is, the small N-valued graph can be extended to an N-valued graph defined on an annulus where the outer radius of the annulus is proportional to R. Here R is the radius of the ball in $\mathbf{R}^3$ in which the boundary of Σ is contained.

C. The N-valued graph not only extends horizontally (i.e., tangent to the initial sheets) but also vertically (i.e., transversally to the sheets). That is, once there are N sheets there are many more and, in fact, the disk Σ consists of two multi-valued graphs glued together along an axis.

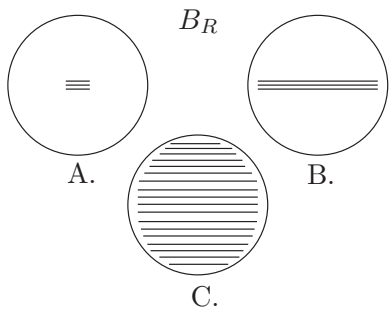

Figure 4: Proving Theorem 0.2.
A. Finding a small N-valued graph in Σ. B. Extending it in Σ to a large N-valued graph. C. Extending the number of sheets.

A will be proved in [CM4], B will be proved in this paper, and C will be proved in [CM5] and [CM6], where we also will establish the regularity of the "axis."

We will now return to the results proved in this paper, i.e., the proof of B above. We show here that if such an embedded minimal disk in $\mathbf{R}^3$ starts off as an almost flat multi-valued graph, then it will remain so indefinitely.

THEOREM 0.3 (see Figure 5). *Given $\tau > 0$, there exist $N, \Omega, \varepsilon > 0$ so that the following hold*:

Let $\Sigma \subset B_{R_0} \subset \mathbf{R}^3$ be an embedded minimal disk with $\partial\Sigma \subset \partial B_{R_0}$. If $\Omega\, r_0 < 1 < R_0/\Omega$ and Σ contains an N-valued graph Σ_g over $D_1 \setminus D_{r_0}$ with gradient $\leq \varepsilon$ and

$$\Sigma_g \subset \{x_3^2 \leq \varepsilon^2 (x_1^2 + x_2^2)\}\,,$$

then Σ contains a 2-valued graph Σ_d over $D_{R_0/\Omega} \setminus D_{r_0}$ with gradient $\leq \tau$ and $(\Sigma_g)^M \subset \Sigma_d$.

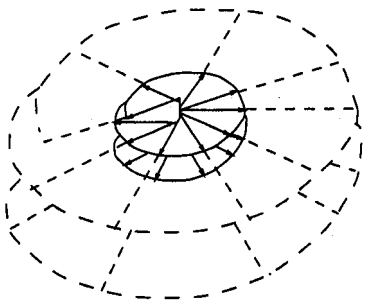

Figure 5: Theorem 0.3 — extending a small multi-valued graph in a disk.

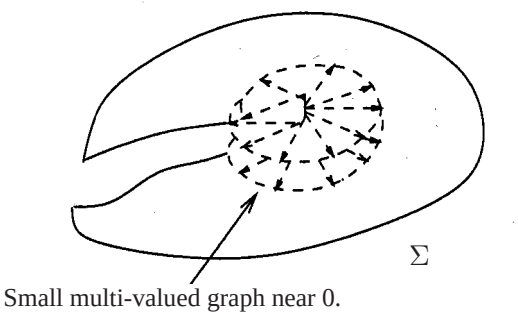

Figure 6: Theorem 0.4— finding a small multi-valued graph in a disk near a point of large curvature.

Theorem 0.3 is particularly useful when combined with a result from [CM4] asserting that an embedded minimal disk with large curvature at a point contains a small, almost flat, multi-valued graph nearby. Namely, we prove in [CM4] the following theorem:

THEOREM 0.4 ([CM4] (see Figure 6)). *Given $N, \omega > 1$, and $\varepsilon > 0$, there exists $C = C(N, \omega, \varepsilon) > 0$ so that the following holds*:

Let $0 \in \Sigma^2 \subset B_R \subset \mathbf{R}^3$ be an embedded minimal disk with $\partial\Sigma \subset \partial B_R$. If for some $0 < r_0 < R$,

$$\sup_{B_{r_0} \cap \Sigma} |A|^2 \leq 4\,|A|^2(0) = 4\,C^2\,r_0^{-2}\,,$$

then there exist $\bar{R} < r_0/\omega$ and (after a rotation of $\mathbf{R}^3$) an N-valued graph $\Sigma_g \subset \Sigma$ over $D_{\omega\bar{R}} \setminus D_{\bar{R}}$ with gradient $\leq \varepsilon$, and $\operatorname{dist}_\Sigma(0, \Sigma_g) \leq 4\,\bar{R}$.

Combining Theorem 0.3 and Theorem 0.4 with a standard blow-up argument gives the following theorem:

THEOREM 0.5 ([CM4]). *Given $N \in \mathbf{Z}_+$, $\varepsilon > 0$, there exist C_1, $C_2 > 0$ so that the following holds*:

Let $0 \in \Sigma^2 \subset B_R \subset \mathbf{R}^3$ be an embedded minimal disk with $\partial\Sigma \subset \partial B_R$. If for some $R > r_0 > 0$,

$$\max_{B_{r_0} \cap \Sigma} |A|^2 \geq 4\,C_1^2\,r_0^{-2}\,,$$

then there exists (after a rotation of $\mathbf{R}^3$) an N-valued graph Σ_g over $D_{R/C_2} \setminus D_{2r_0}$ with gradient $\leq \varepsilon$ and contained in $\Sigma \cap \{x_3^2 \leq \varepsilon^2\,(x_1^2 + x_2^2)\}$.

The multi-valued graphs given by Theorem 0.5 should be thought of (see [CM6]) as the basic building blocks of an embedded minimal disk. In fact, one should think of such a disk as being built out of such graphs by stacking them on top of each other. It will follow from Proposition II.2.12 that the separation between the sheets in such a graph grows sublinearly.

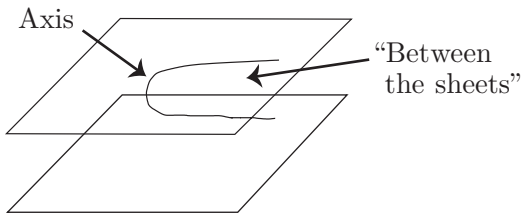

Figure 7: The estimate between the sheets: Theorem I.0.8.

An important component of the proof of Theorem 0.3 is a version of it for stable minimal annuli with slits that start off as multi-valued graphs. Another component is a curvature estimate "between the sheets" for embedded minimal disks in $\mathbf{R}^3$; see Figure 7. We will think of an axis for such a disk Σ as a point or curve away from which the surface locally (in an extrinsic ball) has more than one component. With this weak notion of an axis, our estimate is that if one component of Σ is sandwiched between two others that connect to an axis, then the one that is sandwiched has curvature estimates; see Theorem I.0.8. The example to keep in mind is a helicoid and the components are "consecutive sheets" away from the axis. These separate sheets can be connected along the axis of the helicoid and every component between them must then be graphical and hence have bounded curvature.

Theorems 0.3, 0.4, 0.5 are local and are for simplicity stated and proved only in $\mathbf{R}^3$ although they can with only very minor changes easily be seen to hold for minimal disks in a sufficiently small ball in any given fixed Riemannian 3-manifold.

The paper is divided into 4 parts. In Part I, we show the curvature estimate "between the sheets" when the disk is in a thin slab. In Part II, we show that certain stable disks with interior boundaries starting off as multi-valued graphs remain very flat (cf. Theorem 0.3). This result will be needed, together with Part I, in Part III to generalize the results of Part I to when the disk is not anymore assumed to lie in a slab. Part II will also be used together with Part III, in Part IV to show Theorem 0.3.

Let x_1, x_2, x_3 be the standard coordinates on $\mathbf{R}^3$ and $\Pi : \mathbf{R}^3 \to \mathbf{R}^2$ orthogonal projection to $\{x_3 = 0\}$. For $y \in S \subset \Sigma \subset \mathbf{R}^3$ and $s > 0$, the extrinsic and intrinsic balls and tubes are

(0.6)
$$B_s(y) = \{x \in \mathbf{R}^3 \,|\, |x - y| < s\}\,, \quad T_s(S) = \{x \in \mathbf{R}^3 \,|\, \mathrm{dist}_{\mathbf{R}^3}(x, S) < s\}\,,$$

(0.7) $$\mathcal{B}_s(y) = \{x \in \Sigma \,|\, \mathrm{dist}_\Sigma(x, y) < s\}\,, \mathcal{T}_s(S) = \{x \in \Sigma \,|\, \mathrm{dist}_\Sigma(x, S) < s\}\,.$$

D_s denotes the disk $B_s(0) \cap \{x_3 = 0\}$. K_Σ the sectional curvature of a smooth compact surface Σ and when Σ is immersed A_Σ will be its second fundamental form. When Σ is oriented, $\mathbf{n}_\Sigma$ is the unit normal. We will often consider

the intersection of curves and surfaces with extrinsic balls. We assume that these intersect transversely since this can be achieved by an arbitrarily small perturbation of the radius.

Part I: Minimal disks in a slab

Let $\gamma_{p,q}$ denote the line segment from p to q and $\overline{p,q}$ the ray from p through q. A curve γ is *h-almost monotone* if given $y \in \gamma$, then $B_{4\,h}(y) \cap \gamma$ has only one component which intersects $B_{2\,h}(y)$. Our curvature estimate "between the sheets" is (see Figure 8):

THEOREM I.0.8. *There exist $c_1 \geq 4$ and $2c_2 < c_4 < c_3 \leq 1$ so that the following holds*:

Let $\Sigma^2 \subset B_{c_1\,r_0}$ be an embedded minimal disk with $\partial\Sigma \subset \partial B_{c_1\,r_0}$ and $y \in \partial B_{2\,r_0}$. Suppose that Σ_1, Σ_2, and Σ_3 are distinct components of $B_{r_0}(y) \cap \Sigma$ and

$$\gamma \subset (B_{r_0} \cup T_{c_2\,r_0}(\gamma_{0,y})) \cap \Sigma$$

is a curve with $\partial\gamma = \{y_1, y_2\}$ where $y_i \in B_{c_2\,r_0}(y) \cap \Sigma_i$ and each component of $\gamma \setminus B_{r_0}$ is $c_2\,r_0$-almost monotone.

If Σ_3' is a component of $B_{c_3\,r_0}(y) \cap \Sigma_3$ with y_1, y_2 in distinct components of $B_{c_4\,r_0}(y) \setminus \Sigma_3'$, then Σ_3' is a graph.

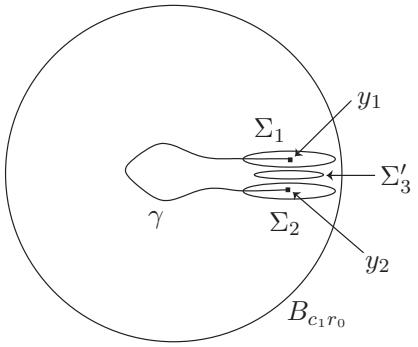

Figure 8: y_1, y_2, Σ_1, Σ_2, Σ_3', and γ in Theorem I.0.8.

The idea for the proof of Theorem I.0.8 is to show that if this were not the case, then we could find an embedded stable disk that would be almost flat and would lie in the complement of the original disk. In fact, we can choose the stable disk to be sandwiched between the two components as well. The flatness would force the stable disk to eventually cross the axis in the original disk, contradicting that they were disjoint.

In this part, we prove Theorem I.0.8 when the surface is in a slab, illustrating the key points (the full theorem, using the results of this part, will be proved later). Two simple facts about minimal surfaces in a slab will be used:

- Stable surfaces in a slab must be graphical away from their boundary (see Lemma I.0.9 below).
- The maximum principle, and catenoid foliations in particular, force these surfaces to intersect a narrow cylinder about every vertical line (see the appendix).

LEMMA I.0.9. *Let $\Gamma \subset \{|x_3| \leq \beta\, h\}$ be a stable embedded minimal surface. There exist $C_g, \beta_s > 0$ so that if $\beta \leq \beta_s$ and E is a component of*

$$\mathbf{R}^2 \setminus T_h(\Pi(\partial\Gamma))\,,$$

then each component of $\Pi^{-1}(E) \cap \Gamma$ is a graph over E of a function u with

$$|\nabla_{\mathbf{R}^2} u| \leq C_g\, \beta\,.$$

Proof. If $\mathcal{B}_h(y) \subset \Gamma$, then the curvature estimate of [Sc] gives

$$\sup_{\mathcal{B}_{h/2}(y)} |A|^2 \leq C_s\, h^{-2}\,.$$

Since $\Delta_\Gamma x_3 = 0$, the gradient estimate of [ChY] yields

$$\sup_{\mathcal{B}_{h/4}(y)} |\nabla_\Gamma x_3| \leq \bar{C}_g\, h^{-1} \sup_{\mathcal{B}_{h/2}(y)} |x_3| \leq \bar{C}_g\, \beta\,, \tag{I.0.10}$$

where $\bar{C}_g = \bar{C}_g(C_s)$. Since

$$|\nabla_{\mathbf{R}^2} u|^2 = |\nabla_\Gamma x_3|^2 \,/\, (1 - |\nabla_\Gamma x_3|^2)\,,$$

(I.0.10) gives the lemma. □

The next lemma shows that if an embedded minimal disk Σ in the intersection of a ball with a thin slab is not graphical near the center, then it contains a curve γ coming close to the center and connecting two boundary points which are close in $\mathbf{R}^3$ but not in Σ. The constant β_A is defined in (A.6).

LEMMA I.0.11. *Let $\Sigma^2 \subset B_{60\,h} \cap \{|x_3| \leq \beta_A\, h\}$ be an embedded minimal disk with $\partial\Sigma \subset \partial B_{60\,h}$ and let $z_b \in \partial B_{50\,h}$. If a component Σ' of $B_{5\,h} \cap \Sigma$ is not a graph, then there are*:

- *Distinct components S_1, S_2 of $B_{8\,h}(z_b) \cap \Sigma$.*
- *Points z_1 and z_2 with $z_i \in B_{h/4}(z_b) \cap S_i$.*
- *A curve $\gamma \subset (B_{30\,h} \cup T_h(\gamma_{q,z_b})) \cap \Sigma$ with $\partial\gamma = \{z_1, z_2\}$ and $\gamma \cap \Sigma' \neq \emptyset$. Here $q \in B_{50\,h}(z_b) \cap \partial B_{30\,h}$.*

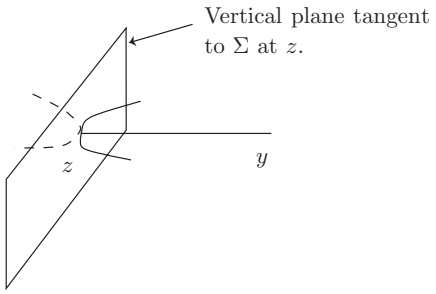

Figure 9: Proof of Lemma I.0.11: Vertical plane tangent to Σ at z. Since Σ is minimal, we get locally near z on one side of the plane two different components. Next place a catenoid foliation centered at y and tangent to Σ at z.

Proof. See Figure 9. Since Σ' is not graphical, we can find $z \in \Sigma'$ with Σ vertical at z, i.e.,

$$|\nabla_\Sigma x_3|(z) = 1\,.$$

Fix a point $y \in \partial B_{4\,h}(z)$ so that $\gamma_{y,z}$ is normal to Σ at z. Then $f_y(z) = 4\,h$ (see (A.5)). Let y' be given such that $y' \in \partial B_{10\,h}(y)$ and $z \in \gamma_{y,y'}$. The first step is to use the catenoid foliation f_y to build the desired curve on the scale of h; see Figure 10. The second and third steps will bring the endpoints of this curve out near z_b.

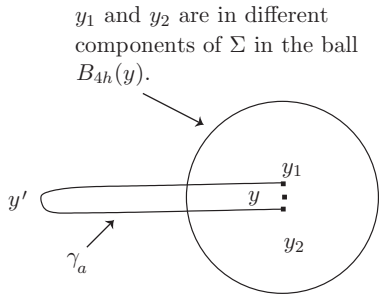

Figure 10: Proof of Lemma I.0.11: Step 1: Using the catenoid foliation, we build out the curve to scale h.

Any simple closed curve $\sigma \subset \Sigma \setminus \{f_y > 4\,h\}$ bounds a disk $\Sigma_\sigma \subset \Sigma$. By Lemma A.8, f_y has no maxima on $\Sigma_\sigma \cap \{f_y > 4\,h\}$ so that we conclude $\Sigma_\sigma \cap \{f_y > 4\,h\} = \emptyset$. On the other hand, by Lemma A.7, we get a neighborhood $U_z \subset \Sigma$ of z where $U_z \cap \{f_y = 4\,h\} \setminus \{z\}$ is the union of $2n \geq 4$ disjoint embedded arcs meeting at z. Moreover, $U_z \setminus \{f_y \geq 4\,h\}$ has n components $U_1, \ldots, U_n$ with

$$\overline{U_i} \cap \overline{U_j} = \{z\} \text{ for } i \neq j\,.$$

If a simple curve $\tilde{\sigma}_z \subset \Sigma \setminus \{f_y \geq 4\,h\}$ connects U_1 to U_2, then connecting $\partial\tilde{\sigma}_z$ by a curve in U_z gives a simple closed curve $\sigma_z \subset \Sigma \setminus \{f_y > 4\,h\}$ with $\tilde{\sigma}_z \subset \sigma_z$ and $\sigma_z \cap \{f_y \geq 4\,h\} = \{z\}$. Hence, σ_z bounds a disk $\Sigma_{\sigma_z} \subset \Sigma \setminus \{f_y > 4\,h\}$. By construction, we have

$$U_z \cap \Sigma_{\sigma_z} \setminus \cup_i \overline{U_i} \neq \emptyset\,.$$

This is a contradiction, so we conclude that U_1, U_2 are contained in components $\Sigma^1_{4\,h} \neq \Sigma^2_{4\,h}$ of $\Sigma \setminus \{f_y \geq 4\,h\}$ with $z \in \overline{\Sigma^1_{4\,h}} \cap \overline{\Sigma^2_{4\,h}}$. For $i = 1, 2$, Lemma A.8 and (A.6) give $y^a_i \in B_{h/4}(y) \cap \Sigma^i_{4\,h}$. Corollary A.10 gives $\nu_i \subset T_h(\gamma_{y,y'}) \cap \Sigma$ with $\partial\nu_i = \{y^a_i, y^b_i\}$ where $y^b_i \in B_{h/4}(y')$. There are now two cases:

- If y^b_1 and y^b_2 do not connect in $B_{4\,h}(y') \cap \Sigma$, then take $\gamma_0 \subset B_{5\,h}(y) \cap \Sigma$ from y^a_1 to y^a_2 and set $\gamma_a = \nu_1 \cup \gamma_0 \cup \nu_2$ and $y_i = y^b_i$.
- Otherwise, if $\hat{\gamma}_0 \subset B_{4\,h}(y') \cap \Sigma$ connects y^b_1 and y^b_2, set $\gamma_a = \nu_1 \cup \hat{\gamma}_0 \cup \nu_2$ and $y_i = y^a_i$.

In either case, after possibly switching y and y', we get a curve

$$\gamma_a \subset (T_h(\gamma_{y,y'}) \cup B_{5\,h}(y')) \cap \Sigma$$

with $\partial\gamma_a = \{y_1, y_2\} \subset B_{h/4}(y)$ and $y_i \in S^a_i$ for components $S^a_1 \neq S^a_2$ of $B_{4\,h}(y) \cap \Sigma$. This completes the first step.

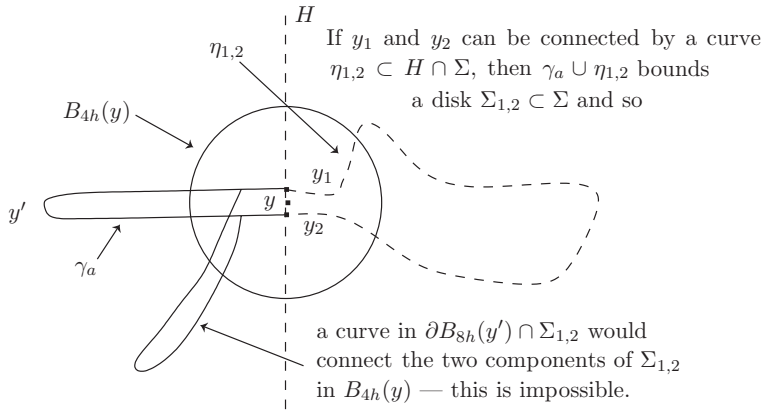

Figure 11: Proof of Lemma I.0.11: Step 2: y_1 and y_2 cannot connect in the half-space H since this would give a point in $\Sigma_{1,2}$ far from $\partial\Sigma_{1,2}$, contradicting Corollary A.10.

Second, we use the maximum principle to restrict the possible curves from y_1 to y_2; see Figure 11. Set

$$H = \{x \,|\, \langle y - y', x - y\rangle > 0\}\,. \tag{I.0.12}$$

If $\eta_{1,2} \subset T_h(H) \cap \Sigma$ connects y_1 and y_2, then $\eta_{1,2} \cup \gamma_a$ bounds a disk $\Sigma_{1,2} \subset \Sigma$. Since $\eta_{1,2} \subset T_h(H)$, we get that $\partial B_{8\,h}(y') \cap \partial\Sigma_{1,2}$ consists of an odd number

of points in each S^a_i and hence $\partial B_{8\,h}(y') \cap \Sigma_{1,2}$ contains a curve from S^a_1 to S^a_2. However, S^a_1 and S^a_2 are distinct components of $B_{4\,h}(y) \cap \Sigma$, so that we conclude this curve contains a point

$$y_{1,2} \in \partial B_{4\,h}(y) \cap \partial B_{8\,h}(y') \cap \Sigma_{1,2}\,. \tag{I.0.13}$$

By construction, $\Pi(y_{1,2})$ is in an unbounded component of $\mathbf{R}^2 \setminus T_{h/4}(\Pi(\partial\Sigma_{1,2}))$, contradicting Corollary A.11. This contradiction shows that y_1 and y_2 cannot be connected in $T_h(H) \cap \Sigma$.

Third, we extend γ_a. There are two cases:

(A) If $z_b \in H$, Corollary A.10 gives

$$\tilde{\nu}_1, \tilde{\nu}_2 \subset T_h(\gamma_{y,z_b}) \cap \Sigma \subset T_h(H) \cap \Sigma \tag{I.0.14}$$

from y_1, y_2 to $z_1, z_2 \in B_{h/4}(z_b)$, respectively.

(B) If $z_b \notin H$, then fix $z_c \in \partial B_{20\,h}(y) \cap \Pi(\partial H)$ on the same side of $\Pi(\overline{y, y'})$ as $\Pi(z_b)$ and fix $z_d \in \partial B_{10\,h}(z_c) \setminus H$ with γ_{z_c,z_d} orthogonal to ∂H (so the four points $\Pi(y'), \Pi(y), z_c, z_d$ form a $10\,h$ by $20\,h$ rectangle). Corollary A.10 gives curves

$$\tilde{\nu}_1, \tilde{\nu}_2 \subset T_h(\gamma_{y,z_c} \cup \gamma_{z_c,z_d} \cup \gamma_{z_d,z_b}) \cap \Sigma \tag{I.0.15}$$

from y_1, y_2 to $z_1, z_2 \in B_{h/4}(z_b)$, respectively.

In either case, set $\gamma = \tilde{\nu}_1 \cup \gamma_a \cup \tilde{\nu}_2$. Set $q = \partial B_{30\,h}(y) \cap \gamma_{y,z_b}$ (in (A)) or $q = \partial B_{30\,h}(y) \cap \gamma_{z_c,z_b}$ (in (B)). By Corollary A.11 as above, z_1, z_2 are in distinct components of $B_{8\,h}(z_b) \cap \Sigma$. □

The next result illustrates the main ideas for Theorem I.0.8 in the simpler case where Σ is in a slab. Set

$$\beta_3 = \min\{\beta_A, \beta_s, \tan\theta_0/(2\,C_g)\};$$

C_g, β_s are defined in Lemma I.0.9, θ_0 in (A.3), and β_A in (A.6).

PROPOSITION I.0.16. *Let $\Sigma \subset B_{4\,r_0} \cap \{|x_3| \leq \beta_3\,h\}$ be an embedded minimal disk with $\partial\Sigma \subset \partial B_{4\,r_0}$ and let $y \in \partial B_{2\,r_0}$. Suppose that $\Sigma_1, \Sigma_2, \Sigma_3$ are distinct components of $B_{r_0}(y) \cap \Sigma$ and*

$$\gamma \subset (B_{r_0} \cup T_h(\gamma_{0,y})) \cap \Sigma$$

is a curve with $\partial\gamma = \{y_1, y_2\}$ where $y_i \in B_h(y) \cap \Sigma_i$ and each component of $\gamma \setminus B_{r_0}$ is h-almost monotone.

If Σ'_3 is a component of $B_{r_0-80\,h}(y) \cap \Sigma_3$ for which y_1, y_2 are in distinct components of $B_{5\,h}(y) \setminus \Sigma'_3$, then Σ'_3 is a graph.

Proof. We will suppose that Σ'_3 is not a graph and deduce a contradiction. Fix a vertical point $z \in \Sigma'_3$. Define z_0, y_0, y_b on the ray $\overline{0, y}$ by

$$\begin{aligned} z_0 &= \partial B_{3\,r_0 - 21\,h} \cap \overline{0, y}\,, \\ y_0 &= \partial B_{3\,r_0 - 10\,h} \cap \overline{0, y}\,, \\ y_b &= \partial B_{4\,r_0} \cap \overline{0, y}\,. \end{aligned}$$

Set $z_b = \partial B_{50\,h}(z) \cap \gamma_{z, z_0}$. Define the half-space

$$H = \{x \,|\, \langle x - z_0, z_0 \rangle > 0\}\,. \tag{I.0.17}$$

The first step is to find a simple curve

$$\gamma_3 \subset (B_{r_0 - 20\,h}(y) \cup T_h(\gamma_{y, y_b})) \cap \Sigma$$

which can be connected to Σ'_3 in $B_{r_0 - 20\,h}(y) \cap \Sigma$, with $\partial\gamma_3 \subset \partial\Sigma$, such that $\partial B_{r_0 - 10\,h}(y) \cap \gamma_3$ consists of an odd number of points in each of two distinct components of $H \cap \Sigma$. To do that, we begin by applying Lemma I.0.11 to get $q \in B_{50\,h}(z_b) \cap \partial B_{30\,h}(z)$, distinct components S_1, S_2 of $B_{8\,h}(z_b) \cap \Sigma$ with $z_i \in B_{h/4}(z_b) \cap S_i$, and a curve

$$\gamma^\star_3 \subset (B_{30\,h}(z) \cup T_h(\gamma_{q, z_b})) \cap \Sigma,\, \partial\gamma^\star_3 = \{z_1, z_2\}\,,\, \gamma^\star_3 \cap \Sigma'_3 \neq \emptyset\,. \tag{I.0.18}$$

Corollary A.10 gives h-almost monotone curves

$$\nu_1\,, \nu_2 \subset T_h(\gamma_{z_b, z_0} \cup \gamma_{z_0, y_b}) \cap \Sigma$$

from z_1, z_2, respectively, to $\partial\Sigma$. Then $\gamma_3 = \nu_1 \cup \gamma^\star_3 \cup \nu_2$ extends $\gamma^\star_3$ to $\partial\Sigma$. Fix points

$$\begin{aligned} z^+ &\in B_h(y_0) \cap \nu_1\,, \\ z^- &\in B_h(y_0) \cap \nu_2\,. \end{aligned}$$

We will show that z^+, z^- do not connect in $H \cap \Sigma$. If $\eta^-_+ \subset H \cap \Sigma$ connects z^+ and z^-, then η^-_+ together with the portion of γ_3 from z^+ to z^- bounds a disk $\Sigma^-_+ \subset \Sigma$. Using the almost monotonicity of each ν_i, we get that $\partial B_{50\,h}(z) \cap \partial\Sigma^-_+$ consists of an odd number of points in each S_i. Consequently, a curve $\sigma^-_+ \subset \partial B_{50\,h}(z) \cap \Sigma^-_+$ connects S_1 to S_2 and so $\sigma^-_+ \setminus B_{8\,h}(z_b) \neq \emptyset$. This would contradict Corollary A.11 and we conclude that there are distinct components Σ^+_H and Σ^-_H of $H \cap \Sigma$ with $z^\pm \in \Sigma^\pm_H$. Finally, removing any loops in γ_3 (so it is simple) gives the desired curve.

The second step is to find disjoint stable disks

$$\Gamma_1, \Gamma_2 \subset B_{r_0 - 2\,h}(y) \setminus \Sigma$$

with $\partial\Gamma_i \subset \partial B_{r_0 - 2\,h}(y)$ and graphical components Γ'_i of $B_{r_0 - 4\,h}(y) \cap \Gamma_i$ so that Σ'_3 is between Γ'_1, Γ'_2 and y_1, y_2, Σ'_3 are each in its own component of

$$B_{r_0 - 4\,h}(y) \setminus (\Gamma'_1 \cup \Gamma'_2)\,.$$

To achieve this, we will solve two Plateau problems using Σ as a barrier and then use the fact that Σ'_3 separates y_1, y_2 near y to get that these are in different components. Let Σ'_1, Σ'_2 be the components of $B_{r_0-2\,h}(y) \cap \Sigma$ with $y_1 \in \Sigma'_1, y_2 \in \Sigma'_2$. By the maximum principle, each of these is a disk. Let Σ_{y_2} be the component of $B_{3\,h}(y_1) \cap \Sigma$ with $y_2 \in \Sigma_{y_2}$. Since $y_1 \notin \Sigma_{y_2}$, Lemma A.8 gives $y'_2 \in \Sigma_{y_2} \setminus N_{\theta_0}(y_1)$ with $\theta_0 > 0$ from (A.3). Hence, the vector $y_1 - y'_2$ is nearly orthogonal to the slab, i.e.,

$$|\Pi(y'_2 - y_1)| \leq |y'_2 - y_1| \cos\theta_0 \,. \tag{I.0.19}$$

Since Σ'_3 separates y_1, y_2 in $B_{5\,h}(y)$, we get $y_3 \in \gamma_{y_1,y'_2} \cap \Sigma'_3$. Fix a component Ω_1 of $B_{r_0-2\,h}(y) \setminus \Sigma$ containing a component of $\gamma_{y_1,y_3} \setminus \Sigma$ with exactly one endpoint in Σ'_1. By [MeYa], we get a stable embedded disk $\Gamma_1 \subset \Omega_1$ with $\partial\Gamma_1 = \partial\Sigma'_1$. Similarly, let Ω_2 be a component of $B_{r_0-2\,h}(y) \setminus (\Sigma \cup \Gamma_1)$ containing a component of $\gamma_{y_3,y'_2} \setminus (\Sigma \cup \Gamma_1)$ with exactly one endpoint in Σ'_2. Again by [MeYa], we get a stable embedded disk $\Gamma_2 \subset \Omega_2$ with $\partial\Gamma_2 = \partial\Sigma'_2$. Since $\partial\Gamma_1, \partial\Gamma_2$ are linked in Ω_1, Ω_2 with (segments of) $\gamma_{y_1,y_3}, \gamma_{y_3,y'_2}$, respectively, we get components Γ'_i of $B_{r_0-4h}(y) \cap \Gamma_i$ with $z_1^\Gamma \in \Gamma'_1 \cap \gamma_{y_1,y_3}$ and $z_2^\Gamma \in \Gamma'_2 \cap \gamma_{y_3,y'_2}$. By Lemma I.0.9, each Γ'_i is a graph of a function u_i with $|\nabla u_i| \leq C_g\,\beta_3$. Hence, since $1 + C_g^2\,\beta_3^2 < 1/\cos^2\theta_0$, we have

$$\Gamma'_i \setminus \{z_i^\Gamma\} \subset N_{\theta_0}(z_i^\Gamma) \,. \tag{I.0.20}$$

By (I.0.19), we have $\gamma_{y_1,y'_2} \cap N_{\theta_0}(z_i^\Gamma) = \emptyset$, so that (I.0.20) implies $\Gamma'_i \cap \gamma_{y_1,y'_2} = \{z_i^\Gamma\}$. In particular, y_1, y_2, y_3 are in distinct components of

$$B_{r_0-4\,h} \setminus (\Gamma'_1 \cup \Gamma'_2) \,.$$

This completes the second step.

Set $\hat{y} = \partial B_{r_0+10\,h} \cap \gamma_{0,y}$. Let $\hat{\gamma}$ be the component of $B_{r_0+10\,h} \cap \gamma$ with $B_{r_0} \cap \hat{\gamma} \neq \emptyset$. Then $\partial\hat{\gamma} = \{\hat{y}_1, \hat{y}_2\}$ with $\hat{y}_i \in B_h(\hat{y}) \cap \Sigma'_i$.

The third step is to solve the Plateau problem with γ_3 together with part of $\partial\Sigma \subset \partial B_{4\,r_0}$ as the boundary to get a stable disk $\Gamma_3 \subset B_{4r_0} \setminus \Sigma$ passing between $\hat{y}_1, \hat{y}_2$. To do this, note that the curve γ_3 divides the disk Σ into two sub-disks Σ_3^+, Σ_3^-. Let Ω^+, Ω^- be the components of $B_{4\,r_0} \setminus (\Sigma \cup \Gamma_1 \cup \Gamma_2)$ with $\gamma_3 \subset \partial\Omega^+ \cap \partial\Omega^-$. Note that Ω^+, Ω^- are mean convex in the sense of [MeYa] since $\partial\Gamma_1 \cup \partial\Gamma_2 \subset \Sigma$ and $\partial\Sigma \subset \partial B_{4\,r_0}$. Using the first step, we can label Ω^+, Ω^- so that the z^+, z^- do not connect in $H \cap \Omega^+$. By [MeYa], we get a stable embedded disk $\Gamma_3 \subset \Omega^+$ with $\partial\Gamma_3 = \partial\Sigma_3^+$. By the almost monotonicity, $\partial B_{r_0-10\,h}(y) \cap \partial\Gamma_3$ consists of an odd number of points in each of Σ_H^+, Σ_H^-. Hence, there is a curve

$$\gamma_+^- \subset \partial B_{r_0-10\,h}(y) \cap \Gamma_3$$

from Σ_H^+ to Σ_H^-. By construction, $\gamma_+^- \setminus B_{8\,h}(y_0) \neq \emptyset$. Hence, since

$$\partial B_{r_0-10\,h}(y) \cap T_h(\partial\Gamma_3) \subset B_{3\,h}(y_0) \,,$$

Lemma I.0.9 gives $\hat{z} \in B_h(\hat{y}_1) \cap \gamma_+^-$. By the second step, Γ_3 is between Γ_1' and Γ_2'.

Let $\hat{\Gamma}_3$ be the component of $B_{r_0+19\,h} \cap \Gamma_3$ with $\hat{z} \in \hat{\Gamma}_3$. By Lemma I.0.9, $\hat{\Gamma}_3$ is a graph. Finally, since $\hat{\gamma} \subset B_{r_0+10\,h}$ and $\hat{\Gamma}_3$ passes between $\partial\hat{\gamma}$, this forces $\hat{\Gamma}_3$ to intersect $\hat{\gamma}$. This contradiction completes the proof. □

Part II. Estimates for stable annuli with slits

In this part, we will show that certain stable disks starting off as multi-valued graphs remain the same (see Theorem II.0.21 below). This is needed in Part III when we generalize the results of Part I to when the surface is not anymore in a slab and in Part IV when we show Theorem 0.3.

THEOREM II.0.21. *Given $\tau > 0$, there exist $N_1, \Omega_1, \varepsilon > 0$ so that the following holds*:

Let $\Sigma \subset B_{R_0}$ be a stable embedded minimal disk with $\partial\Sigma \subset B_{r_0} \cup \partial B_{R_0} \cup \{x_1 = 0\}$ where $\partial\Sigma \setminus \partial B_{R_0}$ is connected. If $\Omega_1\, r_0 < 1 < R_0/\Omega_1$ and Σ contains an N_1-valued graph Σ_g over $D_1 \setminus D_{r_0}$ with gradient $\leq \varepsilon$,

$$\Pi^{-1}(D_{r_0}) \cap \Sigma^M \subset \{|x_3| \leq \varepsilon\, r_0\}\,,$$

and a curve η connects Σ_g to $\partial\Sigma \setminus \partial B_{R_0}$ where

$$\eta \subset \Pi^{-1}(D_{r_0}) \cap \Sigma \setminus \partial B_{R_0}\,,$$

then Σ contains a 2-valued graph Σ_d over $D_{R_0/\Omega_1} \setminus D_{r_0}$ with gradient $\leq \tau$.

Two analytical results go into the proof of this extension theorem. First, we show that if an almost flat multi-valued graph sits inside a stable disk, then the outward defined intrinsic sector from a curve which is a multi-valued graph over a circle has a subsector which is almost flat (see Corollary II.1.23 below). As the initial multi-valued graph becomes flatter and the number of sheets in it go up, the subsector becomes flatter. The second analytical result that we will need is that in a multi-valued minimal graph the distance between the sheets grows sublinearly (Proposition II.2.12).

After establishing these two facts, the first application (Corollary II.3.1) is to extend the middle sheet as a multi-valued graph. This is done by dividing the initial multi-valued graph (or curve in the graph that is itself a multi-valued graph over the circle) into three parts where the middle sheet is the second part. The idea is then that the first and third parts have subsectors which are almost flat multi-valued graphs and the middle part (which has curvature estimates since it is stable) is sandwiched between the two others. Hence its sector is also almost flat.

The proof of the extension theorem is somewhat more complicated than suggested in the above sketch since we must initially assume a bound for the

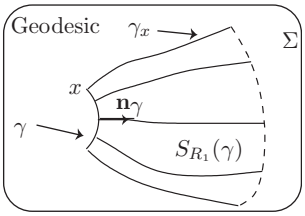

Figure 12: An intrinsic sector over a curve γ defined in (II.0.22).

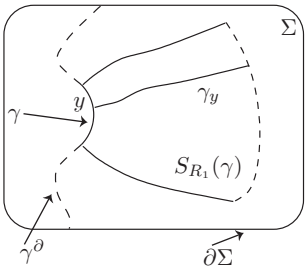

Figure 13: The curve γ^∂ containing γ goes to $\partial\Sigma$. ($\gamma^\partial \setminus \gamma$ is dotted.)

ratio between the size of the initial multi-valued graph and how far out it extends. This is because the flatness of the subsector comes from a total curvature estimate which is in terms of this ratio (see (II.1.2)) and can only be made small by looking at a fixed large number of rotations for the graph. This forces us to successively extend the multi-valued graph. The issue is then to make sure that as we move out in the sector and repeat the argument we have essentially not lost sheets. This is taken care of by using the sublinear growth of the separation between the sheets together with the Harnack inequality (Lemma II.3.8) and the maximum principle (Corollary II.3.1). (The maximum principle is used to make sure, as we try to recover sheets after we have moved out that we do not hit the boundary of the disk before we have recovered essentially all of the sheets that we started with.) The last statement is a result from [CM3] to guarantee as we patch together these multi-valued graphs coming from different scales that the surface obtained is still a multi-valued graph over a fixed plane.

Unless otherwise stated in this part, Σ will be a stable embedded disk. Let $\gamma \subset \Sigma$ be a simple curve with unit normal $\mathbf{n}_\gamma$ and geodesic curvature k_g (with respect to $\mathbf{n}_\gamma$). We will always assume that γ' does not vanish. Given $R_1 > 0$, we define the intrinsic sector (see Figure 12),

$$S_{R_1}(\gamma) = \cup_{x\in\gamma}\gamma_x\,, \tag{II.0.22}$$

where γ_x is the (intrinsic) geodesic starting at $x \in \gamma$, of length R_1, and initial direction $\mathbf{n}_\gamma(x)$. For $0 < r_1 < R_1$, set

$$\begin{aligned} S_{r_1,R_1}(\gamma) &= S_{R_1}(\gamma) \setminus S_{r_1}(\gamma)\,,\\ \rho(x) &= \mathrm{dist}_{S_{R_1}(\gamma)}(x,\gamma)\,. \end{aligned}$$

For example, if $\gamma = \partial D_{r_1} \subset \mathbf{R}^2$ and $\mathbf{n}_\gamma(x) = x/|x|$, then S_{r_2,R_1} is the annulus $D_{R_1+r_1} \setminus D_{r_2+r_1}$.

Note that if $k_g > 0$, $S_{R_1}(\gamma) \cap \partial\Sigma = \emptyset$, and there is a simple curve $\gamma^\partial \subset \Sigma$ with $\gamma \subset \gamma^\partial$, $\partial\gamma^\partial \subset \partial\Sigma$, and $\gamma_x \cap \gamma^\partial = \{x\}$ for any γ_x as above (see Figure 13),

then the normal exponential map from γ (in direction $\mathbf{n}_\gamma$) gives a diffeomorphism to $S_{R_1}(\gamma)$. Namely, by the Gauss-Bonnet theorem, an n-gon in Σ with concave sides and n interior angles $\alpha_i > 0$ has

$$(n-2)\,\pi \geq \sum_{i=1}^{n} \alpha_i - \int k_g \geq \sum_{i=1}^{n} \alpha_i \,. \tag{II.0.23}$$

In particular, $n > 2$ always and if $\sum_i \alpha_i > \pi$, then $n > 3$. Fix $x, y \in \gamma$ and geodesics γ_x, γ_y as above. If γ_x had a self-intersection, then it would contain a simple geodesic loop, contradicting (II.0.23). Similarly, if γ_x were to intersect γ_y, then we would get a concave triangle with $\alpha_1 = \alpha_2 = \pi/2$ (since γ_x, γ_y do not cross γ^∂), contradicting (II.0.23).

Note also that $S_{r_1,R_1}(\gamma) = S_{R_1-r_1}(S_{r_1,r_1}(\gamma))$ for $0 < r_1 < R_1$.

II.1. Almost flat subsectors

We will next show that certain stable sectors contain almost flat subsectors.

LEMMA II.1.1. *Let $\gamma \subset \Sigma$ be a curve with* $\text{Length}(\gamma) \leq 3\,\pi\,m\,r_1$, *geodesic curvature k_g satisfying $0 < k_g < 2/r_1$, and*

$$\text{dist}_\Sigma(S_{R_1}(\gamma), \partial\Sigma) \geq r_1/2\,,$$

where $R_1 > 2\,r_1$. If there is a simple curve $\gamma^\partial \subset \Sigma$ with $\gamma \subset \gamma^\partial$, $\partial\gamma^\partial \subset \partial\Sigma$, and so

$$\gamma_x \cap \gamma^\partial = \{x\} \text{ for each } x \in \gamma\,,$$

then for any $\Omega > 2$ and t satisfying $2\,r_1 \leq t \leq 3R_1/4$,

$$\int_{S_{\Omega r_1, R_1/\Omega}(\gamma)} |A|^2 \leq C_1\,R_1/r_1 + C_2\,m/\log\Omega\,, \tag{II.1.2}$$

$$t\int_\gamma k_g \leq \text{Length}(\{\rho = t\}) \leq C_3\,(m + R_1/r_1)\,t\,. \tag{II.1.3}$$

Proof. The boundary of $S_{R_1} = S_{R_1}(\gamma)$ has four pieces:

$$\gamma,\ \{\rho = R_1\},\ \text{ and the sides } \gamma_a, \gamma_b\,.$$

Define the functions $\ell(t)$ and $K(t)$ by

$$\ell(t) = \text{Length}\left(\{\rho = t\}\right), \tag{II.1.4}$$

$$K(t) = \int_{S_t} |A|^2\,. \tag{II.1.5}$$

Since the exponential map is an embedding, an easy calculation gives

$$\ell'(t) = \int_{\{\rho=t\}} k_g > 0\,. \tag{II.1.6}$$

Let $d\mu$ be 1-dimensional Hausdorff measure on the level sets of ρ. The Jacobi equation gives

$$\frac{d}{dt}(k_g\, d\mu) = |A|^2/2\, d\mu\,. \tag{II.1.7}$$

Define $\bar{K}(t)$ to be the integral of $K(t)$, i.e., set

$$\bar{K}(t) = \int_0^t K(s)\, ds\,.$$

Integrating (II.1.7) twice, we see that (II.1.6) yields

$$\begin{aligned}\ell(t) &= \ell(0) + \int_0^t \left(\int_\gamma k_g + K(s)/2\right) ds \\ &= \text{Length}(\gamma) + t\int_\gamma k_g + \bar{K}(t)/2\,. \end{aligned}\tag{II.1.8}$$

This gives the first inequality in (II.1.3). Again by the co-area formula, (II.1.8) gives

$$\begin{aligned} R_1^{-2}\,\text{Area}(S_{R_1}) = R_1^{-2}\int_0^{R_1}\ell(t) &\le R_1^{-1}\,\text{Length}(\gamma) + \int_\gamma k_g/2 + R_1^{-2}\int_0^{R_1}\bar{K}(t)/2 \\ &\le 6\,\pi\, m + R_1^{-2}\int_0^{R_1}\bar{K}(t)/2\,, \end{aligned}\tag{II.1.9}$$

where the last inequality used $k_g < 2/r_1$ on γ, $\text{Length}(\gamma) \le 3\,\pi\, m\, r_1$, and $R_1 > 2\, r_1$.

Define a function ψ on S_{R_1} by

$$\psi = \psi(\rho) = 1 - \rho/R_1$$

and set $d_S = \text{dist}_\Sigma(\cdot, \gamma_a \cup \gamma_b)$. Define functions χ_1, χ_2 on S_{R_1} by

$$\chi_1 = \chi_1(d_S) = \begin{cases} d_S/r_1 & \text{if } 0 \le d_S \le r_1\,, \\ 1 & \text{otherwise}\,, \end{cases} \tag{II.1.10}$$

$$\chi_2 = \chi_2(\rho) = \begin{cases} \rho/r_1 & \text{if } 0 \le \rho \le r_1\,, \\ 1 & \text{otherwise}\,. \end{cases} \tag{II.1.11}$$

Set $\chi = \chi_1\,\chi_2$. Using the curvature estimate $|A|^2 \le C\, r_1^{-2}$ (by [Sc]) and standard comparison theorems to bound the area of a tubular neighborhood of the boundary, we get

$$\text{Area}(S_{R_1} \cap \{\chi < 1\}) \le \tilde{C}\,(R_1\, r_1 + m\, r_1^2)\,, \tag{II.1.12}$$

$$E(\chi_1) + \int_{S_{R_1}\cap\{\chi_1<1\}} |A|^2 \le \tilde{C}\, R_1/r_1\,, \tag{II.1.13}$$

$$E(\chi) + \int_{S_{R_1}\cap\{\chi<1\}} |A|^2 \le \tilde{C}\,(R_1/r_1 + m)\,. \tag{II.1.14}$$

Substitution of $\chi\psi$ into the stability inequality, the Cauchy-Schwarz inequality and (II.1.14) give

$$\int |A|^2\chi^2\psi^2 \leq \int |\nabla(\chi\psi)|^2 = \int \left(\chi^2|\nabla\psi|^2 + 2\chi\,\psi\langle\nabla\chi,\nabla\psi\rangle + \psi^2|\nabla\chi|^2\right)$$

$$\leq 2\int \chi^2|\nabla\psi|^2 + 2\,\tilde{C}(R_1/r_1 + m)\,. \tag{II.1.15}$$

Using (II.1.14) and the co-area formula, we have

$$\int_0^{R_1} \psi^2(t)\,K'(t) = \int_{S_{R_1}} |A|^2\psi^2 \leq \int |A|^2\chi^2\psi^2 + \tilde{C}\,(R_1/r_1 + m)\,. \tag{II.1.16}$$

Integration by parts twice in (II.1.16), (II.1.15) gives

$$2\,R_1^{-2}\int_0^{R_1} \bar{K}(t) = \int_0^{R_1} \bar{K}(t)(\psi^2)'' = -\int_0^{R_1} K(t)(\psi^2)'$$

$$= \int_0^{R_1} \psi^2 K'(t) \leq 3\,\tilde{C}\,(R_1/r_1 + m) + 2R_1^{-2}\int_0^{R_1} \ell(t)\,. \tag{II.1.17}$$

Note that all integrals in (II.1.17) are in one variable and there is a slight abuse of notation with regard to ψ as a function on both $[0, R_1]$ and S_{R_1}. Substitution of (II.1.9), (II.1.17) gives

$$4\,R_1^{-2}\int_0^{R_1} \ell(t) \leq 24\,\pi\,m + 3\,\tilde{C}\,(R_1/r_1 + m) + 2\,R_1^{-2}\int_0^{R_1} \ell(t)\,. \tag{II.1.18}$$

In particular, (II.1.18) gives

$$R_1^{-2}\mathrm{Area}(S_{R_1}) \leq C_4\,(R_1/r_1 + m)\,. \tag{II.1.19}$$

Since $\ell(t)$ is monotone increasing (by (II.1.6)), (II.1.19) gives the second inequality in (II.1.3) for $t = 3\,R_1/4$. Since the above argument applies with R_1 replaced by t where $2\,r_1 < t < R_1$, we get (II.1.3) for $2\,r_1 \leq t \leq 3\,R_1/4$.

To complete the proof, we will use the stability inequality together with the logarithmic cutoff trick to take advantage of the quadratic area growth. Define a cutoff function ψ_1 by

$$\psi_1 = \psi_1(\rho) = \begin{cases} \log(\rho/r_1)/\log\Omega & \text{on } S_{r_1,\Omega\,r_1}\,, \\ 1 & \text{on } S_{\Omega\,r_1,R_1/\Omega}\,, \\ -\log(\rho/R_1)/\log\Omega & \text{on } S_{R_1/\Omega,R_1}\,, \\ 0 & \text{otherwise}\,. \end{cases} \tag{II.1.20}$$

Using (II.1.3) and (II.1.19), we get

$$E(\psi_1) \leq C(m + R_1/r_1)/\log\Omega\,. \tag{II.1.21}$$

As in (II.1.15), we apply the stability inequality to $\chi_1\psi_1$ to get

(II.1.22)
$$\int |A|^2\chi_1^2\psi_1^2 \leq 2E(\psi_1) + 2E(\chi_1) \leq 2\,C(m + R_1/r_1)/\log\Omega + 2\tilde{C}\,R_1/r_1\,.$$

Combination of (II.1.13) and (II.1.22) completes the proof. □

The next corollary uses Lemma II.1.1 to show that large stable sectors have almost flat subsectors:

COROLLARY II.1.23. *Given $\omega > 8, 1 > \varepsilon > 0$, there exist m_1, Ω_1 so that the following holds*:

Suppose $\gamma \subset B_{2\,r_1} \cap \Sigma$ is a curve with $1/(2\,r_1) < k_g < 2/r_1$, $\text{Length}(\gamma) = 32\,\pi\,m_1\,r_1$, $\text{dist}_\Sigma(S_{\Omega_1^2\,\omega\,r_1}(\gamma), \partial\Sigma) \geq r_1/2$. If there is a simple curve $\gamma^\partial \subset \Sigma$ with $\gamma \subset \gamma^\partial$, $\partial\gamma^\partial \subset \partial\Sigma$, and

$$\gamma_x \cap \gamma^\partial = \{x\} \text{ for each } x \in \gamma\,,$$

then (after a rotation of $\mathbf{R}^3$) $S_{\Omega_1^2\,\omega\,r_1}(\gamma)$ contains a 2-valued graph Σ_d over $D_{2\,\omega\,\Omega_1\,r_1}\backslash D_{\Omega_1\,r_1/2}$ with gradient $\leq \varepsilon/2$, $|A| \leq \varepsilon/(2\,r)$, and $\text{dist}_{S_{\Omega_1^2\,\omega\,r_1}(\gamma)}(\gamma, \Sigma_d) < 2\,\Omega_1\,r_1$.

Proof. We will choose $\Omega_1 > 12$ and then set $m_1 = \omega\,\Omega_1^2\,\log\Omega_1$. By Lemma II.1.1 (with $\Omega = \Omega_1/6$, $R_1 = \Omega_1^2\,\omega\,r_1$, and $m = 32\,m_1/3$),

$$\int_{S_{\Omega_1\,r_1/6, 6\,\Omega_1\,\omega\,r_1}(\gamma)} |A|^2 \leq C(\Omega_1^2\,\omega + m_1/\log\Omega_1) = 2\,C\,m_1/\log\Omega_1\,. \tag{II.1.24}$$

Fix m_1 disjoint curves $\gamma_1, \ldots, \gamma_{m_1} \subset \gamma$ with $\text{Length}(\gamma_i) = 32\,\pi\,r_1$. By (II.1.24) and since the $S_{\Omega_1^2\,\omega\,r_1}(\gamma_i)$ are pairwise disjoint, there exists γ_i with

$$\int_{S_{\Omega_1\,r_1/6, 6\,\Omega_1\,\omega\,r_1}(\gamma_i)} |A|^2 \leq 2\,C/\log\Omega_1\,. \tag{II.1.25}$$

To deduce the corollary from (II.1.25) we need a few standard facts. First, define a map

$$\Phi : [0, \Omega_1^2\omega r_1] \times_{\rho/(2\,r_1)+1} [0, \text{Length}(\gamma)] \to \Sigma$$

by $\Phi(\rho, x) = \gamma_x(\rho)$. By the Riccati comparison argument (using $\text{K}_\Sigma \leq 0$ and $k_g > 1/(2\,r_1)$ on γ),

$$\Phi \text{ is distance nondecreasing and } k_g > \frac{1}{\rho + 2\,r_1}\,. \tag{II.1.26}$$

Second, let $\gamma_i/2 \subset \gamma_i$ be the subcurve of length $16\,\pi\,r_1$ with $\text{dist}_\gamma(\gamma_i/2, \partial\gamma_i) = 8\,\pi\,r_1$. Since $k_g > 1/(2\,r_1)$ on γ, we have $\int_{\gamma_i/2} k_g > 8\,\pi$. By (II.1.7),

$$\int_{S_{\Omega_1^2\,\omega\,r_1}(\gamma_i/2)\cap\{\rho=t\}} k_g$$

is a monotone nondecreasing function of t. In particular, we can choose a curve $\tilde{\gamma} \subset \gamma_i/2$ with

$$\int_{S_{\Omega_1^2\,\omega\,r_1}(\tilde{\gamma})\cap\{\rho=\Omega_1\,r_1/3\}} k_g = 8\,\pi\,. \tag{II.1.27}$$

Set $S = S_{\Omega_1\,r_1/3,3\,\Omega_1\,\omega\,r_1}(\tilde{\gamma})$ and $\hat{\gamma} = S \cap \{\rho = \Omega_1\,r_1/3\}$.

Third, by the Gauss-Bonnet theorem, (II.1.25), and (II.1.27) (for Ω_1 large),

$$8\,\pi \leq \int_{S\cap\{\rho=t\}} k_g \leq 8\,\pi + \int_S |A|^2/2 \leq 8\,\pi + C/\log\Omega_1 \leq 9\,\pi\,. \tag{II.1.28}$$

Note also that, by (II.1.26) and (II.1.28),

$$\text{Length}(S \cap \{\rho = t\}) \leq 9\,\pi\,(t + 2\,r_1) \leq 14\,\pi\,t\,.$$

Finally, observe that, by stability, (II.1.25), and by (II.1.26), the mean value theorem gives for $y \in S$

$$\sup_{\mathcal{B}_{\rho(y)/3}(y)} |A|^2 \leq C_1\,\rho^{-2}(y)/\log\Omega_1\,. \tag{II.1.29}$$

Integrating (II.1.29) along rays and level sets of ρ, we get

$$\max_{x,y\in S} \text{dist}_{\mathbf{S}^2}(\mathbf{n}(x),\mathbf{n}(y)) \leq C_2\,(\log\omega + 1)/\sqrt{\log\Omega_1}\,. \tag{II.1.30}$$

We can now combine these facts to prove the corollary. Choose Ω_1 so that

$$C_2\,(\log\omega + 1)/\sqrt{\log\Omega_1} < C_3\,\varepsilon\,.$$

For C_3 small, after rotating $\mathbf{R}^3$, S is locally a graph over $\{x_3 = 0\}$ with gradient $\leq \varepsilon/2$. Since $\tilde{\gamma} \subset B_{2\,r_1}$ and $\Omega_1 > 12$,

$$\hat{\gamma} \subset B_{2\,r_1+\Omega_1\,r_1/3} \subset B_{\Omega_1\,r_1/2}\,.$$

Choosing Ω_1 even larger and combining (II.1.26), (II.1.28), (II.1.29), and (II.1.30), we see that (the orthogonal projection) $\Pi(\hat{\gamma})$ is a convex planar curve with total curvature at least $7\,\pi$, so that its Gauss map covers $\mathbf{S}^1$ three times. Given $x \in \tilde{\gamma}$, set $\tilde{\gamma}_x = S \cap \gamma_x$. By (II.1.29), $\tilde{\gamma}_x$ has total (extrinsic geodesic) curvature at most

$$C_2\,\log\omega/\sqrt{\log\Omega_1} < C_3\,\varepsilon$$

and hence $\tilde{\gamma}_x$ lies in a narrow cone centered on its tangent ray at $\tilde{x} = \tilde{\gamma}_x \cap \hat{\gamma}$. For C_3 small, this implies that $\tilde{\gamma}_x$ does not rotate and

$$|\Pi(\tilde{x}) - \Pi(\tilde{\gamma}_x \cap \{\rho = t\})| \geq 9\,(t - \Omega_1\,r_1/3)/10\,. \tag{II.1.31}$$

Hence, $\Pi(\partial\tilde{\gamma}_x \setminus \{\tilde{x}\}) \notin D_{2\,\omega\,\Omega_1\,r_1}$ which gives Σ_d and also $\text{dist}_{S_{\Omega_1^2\,\omega\,r_1}(\gamma)}(\gamma,\Sigma_d) < 2\,\Omega_1\,r_1$. □

REMARK II.1.32. For convenience, we assumed that $k_g < 2/r_1$ in Corollary II.1.23. This was used only to apply Lemma II.1.1 and it was used there only to bound $\int_\gamma k_g$ in (II.1.9).

Recall that a domain Ω is 1/2-stable if and only if, for all $\phi \in C_0^{0,1}(\Omega)$, there exists the 1/2-stability inequality:

$$1/2 \int |A|^2 \phi^2 \leq \int |\nabla \phi|^2 \,. \tag{II.1.33}$$

Note that the interior curvature estimate of [Sc] extends to 1/2-stable surfaces.

In light of Remark II.1.32, it is easy to get the following analog of Corollary II.1.23:

COROLLARY II.1.34. *Given $\omega > 8, 1 > \varepsilon > 0, C_0$, and N, there exist m_1, Ω_1 so that the following holds*:

Suppose that Σ is an embedded minimal disk and $\gamma \subset \partial \mathcal{B}_{r_1}(y) \subset \Sigma$ is a curve with

$$\int_\gamma k_g < C_0 \, m_1 \text{ and } \text{Length}(\gamma) = m_1 \, r_1 \,.$$

If $\mathcal{T}_{r_1/8}(S_{\Omega_1^2 \, \omega \, r_1}(\gamma))$ is 1/2-stable, then (after rotating $\mathbf{R}^3$) $S_{\Omega_1^2 \, \omega \, r_1}(\gamma)$ contains an N-valued graph Σ_N over $D_{\omega \, \Omega_1 \, r_1} \setminus D_{\Omega_1 \, r_1}$ with gradient $\leq \varepsilon$, $|A| \leq \varepsilon / r$, and

$$\text{dist}_{S_{\Omega_1^2 \, \omega \, r_1}(\gamma)}(\gamma, \Sigma_N) < 4 \, \Omega_1 \, r_1 \,.$$

Note that, in Corollary II.1.34, both $k_g \geq 1/r_1$ and the injectivity of the exponential map follow immediately from comparison theorems.

II.2. The sublinear growth

This section gives an elementary gradient estimate for multi-valued minimal graphs which is applied to show that the separation between the sheets of certain minimal graphs grows sublinearly; see Figure 14. The example to keep in mind is the portion of a (rescaled) helicoid in a slab between two cylinders about the vertical axis. This gives (two) multi-valued graphs over an annulus; removal of a vertical half-plane through the axis cuts these into sheets which remain a bounded distance apart.

The next lemma and corollary construct the cutoff function needed in our gradient estimate.

LEMMA II.2.1. *Given $N > 36/(1 - \mathrm{e}^{-1/3})^2$, there exists a function $0 \leq \phi \leq 1$ on $\mathcal{P}$ with $E(\phi) \leq 4 \, \pi / \log N$ and*

$$\phi = \begin{cases} 1 & \text{if } R/\mathrm{e} \leq \rho \leq \mathrm{e} \, R \text{ and } |\theta| \leq 3 \, \pi \,, \\ 0 & \text{if } \rho \leq \mathrm{e}^{-N} \, R \text{ or } \mathrm{e}^N \, R \leq \rho \text{ or } |\theta| \geq \pi \, N \,. \end{cases} \tag{II.2.2}$$

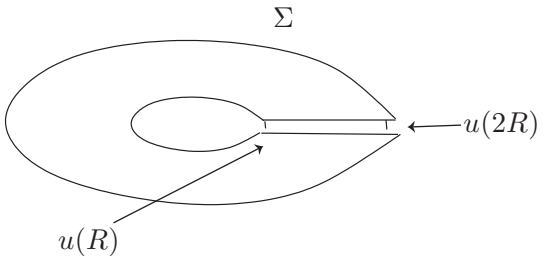

Figure 14: The sublinear growth of the separation u of the multi-valued graph Σ: $u(2R) \leq 2^{\alpha}\, u(R)$ with $\alpha < 1$.

Proof. After rescaling, we may assume that $R = 1$. Since energy is conformally invariant on surfaces, composing with $z^{3\,N}$ implies that (II.2.2) is equivalent to $E(\phi) \leq 4\,\pi/\log N$ and

$$\phi = \begin{cases} 1 & \text{if } |\log \rho| < 1/(3\,N) \text{ and } |\theta| \leq \pi/N\,, \\ 0 & \text{if } |\log \rho| > 1/3 \text{ or } |\theta| \geq \pi/3\,. \end{cases} \tag{II.2.3}$$

This is achieved (with $E(\phi) = 2\,\pi/\log[N(1-\mathrm{e}^{-1/3})/6]$) by setting

$$\phi = \begin{cases} 1 & \text{on } \mathcal{B}_{6/N}(1,0)\,, \\ 1 - \frac{\log[N\,\mathrm{dist}_{\mathcal{P}}((1,0),\cdot)/6]}{\log[N(1-\mathrm{e}^{-1/3})/6]} & \text{on } \mathcal{B}_{1-\mathrm{e}^{-1/3}}(1,0) \setminus \mathcal{B}_{6/N}(1,0)\,, \\ 0 & \text{otherwise}\,. \end{cases} \tag{II.2.4}$$

□

Given an N-valued graph Σ, let $\Sigma^{\theta_1,\theta_2}_{r_3,r_4} \subset \Sigma$ be the subgraph (cf. (0.1)) over

$$\{(\rho,\theta)\,|\,r_3 \leq \rho \leq r_4,\, \theta_1 \leq \theta \leq \theta_2\}\,. \tag{II.2.5}$$

Transplanting the cutoff function from Lemma II.2.1 to a multi-valued graph gives the next corollary:

COROLLARY II.2.6. *Given $\varepsilon_0, \tau > 0$, there exists $N > 0$ so if $\Sigma \subset \mathbf{R}^3$ is an N-valued graph over $D_{\mathrm{e}^N\,R} \setminus D_{\mathrm{e}^{-N}\,R}$ with gradient $\leq \tau$, then there is a cutoff function $0 \leq \phi \leq 1$ on Σ with $E(\phi) \leq \varepsilon_0$, $\phi|_{\partial\Sigma} = 0$, and*

$$\phi \equiv 1 \text{ on } \Sigma^{-\pi,3\pi}_{R/2,5R/2}\,. \tag{II.2.7}$$

Proof. Since $\Sigma^{-\pi,3\pi}_{R/2,5R/2} \subset \Sigma^{-3\pi,3\pi}_{R/\mathrm{e},\mathrm{e}R}$ and the projection from Σ to $\mathcal{P}$ is bi-Lipschitz with bi-Lipschitz constant bounded by $\sqrt{1+\tau^2}$, the corollary follows from Lemma II.2.1. □

If $u > 0$ is a solution of the Jacobi equation $\Delta u = -|A|^2 u$ on Σ, then $w = \log u$ satisfies

$$\Delta w = -|\nabla w|^2 - |A|^2 \,. \tag{II.2.8}$$

The Bochner formula, (II.2.8), $\mathrm{K}_\Sigma = -|A|^2/2$, and the Cauchy-Schwarz inequality give

$$\begin{aligned} \Delta |\nabla w|^2 &= 2\,|\mathrm{Hess}_w|^2 + 2\langle \nabla w, \nabla \Delta w\rangle - |A|^2\,|\nabla w|^2 \\ &\geq 2\,|\mathrm{Hess}_w|^2 - 4\,|\nabla w|^2\,|\mathrm{Hess}_w| - 4\,|\nabla w|\,|A|\,|\nabla A| - |A|^2\,|\nabla w|^2 \\ &\geq -2\,|\nabla w|^4 - 3\,|A|^2\,|\nabla w|^2 - 2\,|\nabla A|^2 \,. \end{aligned} \tag{II.2.9}$$

Since the Jacobi equation is the linearization of the minimal graph equation over Σ, analogs of (II.2.8) and (II.2.9) hold for solutions of the minimal graph equation over Σ. In particular, standard calculations give the following analog of (II.2.8):

LEMMA II.2.10. *There exists $\delta_g > 0$ so that if Σ is minimal and u is a positive solution of the minimal graph equation over Σ (i.e., $\{x + u(x)\,\mathbf{n}_\Sigma(x) \,|\, x \in \Sigma\}$ is minimal) with*

$$|\nabla u| + |u|\,|A| \leq \delta_g \,,$$

then $w = \log u$ satisfies, on Σ,

$$\Delta w = -|\nabla w|^2 + \mathrm{div}(a\nabla w) + \langle \nabla w, a \nabla w\rangle + \langle b, \nabla w\rangle + (c-1)|A|^2 \,, \tag{II.2.11}$$

for functions a_{ij}, b_j, c on Σ with $|a|, |c| \leq 3\,|A|\,|u| + |\nabla u|$ and $|b| \leq 2\,|A|\,|\nabla u|$.

The following gives an improved gradient estimate, and consequently an improved bound for the growth of the separation between the sheets, for multi-valued minimal graphs:

PROPOSITION II.2.12. *Given $\alpha > 0$, there exist $\delta_p > 0, N_g > 5$ so that the following holds*:

If Σ is an N_g-valued minimal graph over $D_{\mathrm{e}^{N_g}R} \setminus D_{\mathrm{e}^{-N_g}R}$ with gradient ≤ 1 and $0 < u < \delta_p R$ is a solution of the minimal graph equation over Σ with $|\nabla u| \leq 1$, then for $R \leq s \leq 2R$

$$\sup_{\Sigma^{0,2\pi}_{R,2R}} |A_\Sigma| + \sup_{\Sigma^{0,2\pi}_{R,2R}} |\nabla u|/u \leq \alpha/(4R) \,, \tag{II.2.13}$$

$$\sup_{\Sigma^{0,2\pi}_{R,s}} u \leq (s/R)^\alpha \sup_{\Sigma^{0,2\pi}_{R,R}} u \,. \tag{II.2.14}$$

Proof. Fix $\varepsilon_E > 0$ (to be chosen depending only on α). Corollary II.2.6 gives N (depending only on ε_E) and a function $0 \leq \phi \leq 1$ with compact support on $\Sigma^{-N\pi, N\pi}_{\mathrm{e}^{-N}R, \mathrm{e}^N R}$

$$E(\phi) \leq \varepsilon_E \text{ and } \phi \equiv 1 \text{ on } \Sigma^{-\pi, 3\pi}_{R/2, 5R/2} \,. \tag{II.2.15}$$

Set $N_g = N+1$, so that $\text{dist}_\Sigma(\Sigma^{-N\pi,N\pi}_{\mathrm{e}^{-N}R,\mathrm{e}^N R}, \partial\Sigma) > \mathrm{e}^{-N}R/2$ and hence $|A| \leq C\mathrm{e}^N/R$ on $\Sigma^{-N\pi,N\pi}_{\mathrm{e}^{-N}R,\mathrm{e}^N R}$. Now fix $x \in \Sigma^{0,2\pi}_{R,2R}$. When we substitute ϕ into the stability inequality, (II.2.15) bounds the total second fundamental form of $\Sigma^{-\pi,3\pi}_{R/2,5R/2}$ by ε_E. Hence, by elliptic estimates for the minimal graph equation,

$$\sup_{\mathcal{B}_{3\,R/8}(x)} (R^2\,|\nabla A_\Sigma|^2 + |A_\Sigma|^2) \leq C\,\varepsilon_E R^{-2}\,. \tag{II.2.16}$$

Since Σ and the graph of u are (locally) graphs with bounded gradient, it is easy to see that

$$\sup_{\Sigma^{-N\pi,N\pi}_{\mathrm{e}^{-N}R,\mathrm{e}^N R}} |\nabla u| \leq C\,\mathrm{e}^N \sup_\Sigma |u|/R \leq C\,\mathrm{e}^N\,\delta_p\,. \tag{II.2.17}$$

Set $w = \log u$. Choose $\delta_p > 0$ (depending only on N), so that (II.2.17) implies that w satisfies (II.2.11) on $\Sigma^{-N\pi,N\pi}_{\mathrm{e}^{-N}R,\mathrm{e}^N R}$ with

$$|a|, |b|/|A|, |c| \leq 1/4\,.$$

Applying Stokes' theorem to

$$\mathrm{div}(\phi^2\nabla w - \phi^2 a\nabla w)$$

and using the absorbing inequality, we see that

$$\int_{\mathcal{B}_{R/2}(x)} |\nabla w|^2 \leq \int \phi^2 |\nabla w|^2 \leq C\,E(\phi) \leq C\,\varepsilon_E\,. \tag{II.2.18}$$

When we combine (II.2.11) and (II.2.16), an easy calculation (as in (II.2.9)) shows that on $\mathcal{B}_{3R/8}(x)$

$$\Delta|\nabla w|^2 \geq -C\,|\nabla w|^4 - C\,\varepsilon_E\,R^{-2}\,|\nabla w|^2 - C\,\varepsilon_E\,R^{-4}\,. \tag{II.2.19}$$

By the rescaling argument of [CiSc] (and by the meanvalue inequality), (II.2.18) and (II.2.19) imply a pointwise bound for $|\nabla w|^2$ on $\mathcal{B}_{R/4}(x)$; combining this with (II.2.16) gives (II.2.13) for ε_E small. Integrating (II.2.13) and using the elementary inequality

$$(s-R)/R \leq 2\,\log(s/R)\,,$$

we get (II.2.14). □

II.3. Extending multi-valued graphs in stable disks

Throughout this section $\Sigma \subset B_{R_0}$ is a stable embedded minimal disk with

$$\partial\Sigma \subset B_{r_0} \cup \partial B_{R_0} \cup \{x_1 = 0\}$$

and $\partial\Sigma \setminus \partial B_{R_0}$ connected. Fix a constant τ_k with $0 < \tau_k < 1/4$ so that if Σ_g is a multi-valued minimal graph over $D_{2R} \setminus D_{R/2}$ with gradient $\leq \tau_k$, then $\Pi^{-1}(\partial D_R) \cap \Sigma_g$ has geodesic curvature k_g satisfying

$$1/(2\,R) < k_g < 2/R$$

(with respect to the outward normal).

The next corollary shows that for certain such Σ containing multi-valued graphs, the middle sheet Σ^M extends to a larger scale. The main point is to apply Corollary II.1.23 to get two 2-valued graphs on a larger scale with Σ^M pinched between them. We first use the convex hull property to construct the curves γ_j^∂ needed for Corollary II.1.23.

COROLLARY II.3.1. *Given $\omega, m > 1$, $1/4 \geq \varepsilon > 0$, there exist Ω_1, m_0, δ so that for r_0, r_2, R_2, R_0 with $4\,\Omega_1\, r_0 \leq 4\,\Omega_1\, r_2 < R_2 < R_0/(4\,\Omega_1\,\omega)$ the following holds*:

Let $\Sigma_g \subset \Sigma$ be an m_0-valued graph over $D_{R_2} \setminus D_{r_2}$ with gradient $\leq \tau_k$, separation between the top and bottom sheets $\leq \delta\, R_2$ over ∂D_{R_2}, and

$$\Pi^{-1}(D_{r_2}) \cap \Sigma_g \subset \{|x_3| \leq r_2/2\}\,.$$

If a curve $\eta \subset \Pi^{-1}(D_{r_2}) \cap \Sigma \setminus \partial B_{R_0}$ connects Σ_g to

$$\partial\Sigma \setminus \partial B_{R_0}\,,$$

then Σ^M extends to an m-valued graph over $D_{\omega\, R_2} \setminus D_{r_2}$ with gradient ≤ 1 and $|A| \leq \varepsilon/r$ over $D_{\omega\, R_2} \setminus D_{R_2}$.

Proof. First, we set up the notation. Let $\Omega_1, m_1 > 1$ be given by Corollary II.1.23. Assume that $\Omega_1^2\,\omega, m, m_1 \in \mathbf{Z}$. Set

$$\begin{aligned} m_0 &= 24\,\Omega_1^2\,\omega + 32\,m_1 + m + 1\,,\\ \gamma &= \Pi^{-1}(\partial D_{R_2/\Omega_1}) \cap \Sigma_g\,. \end{aligned}$$

Since $\Pi^{-1}(D_{r_2}) \cap \Sigma_g \subset \{|x_3| \leq r_2/2\}$, the gradient bound gives, for $r_2 \leq R \leq R_2$,

$$\max_{\Pi^{-1}(\partial D_R)\cap\Sigma_g} |x_3| \leq r_2/2 + \tau_k\,(R - r_2) \leq R/2\,, \tag{II.3.2}$$

so that $\gamma \subset B_{2R_2/\Omega_1}$. By the definition of τ_k, we have $\Omega_1/(2\,R_2) < k_g < 2\,\Omega_1/R_2$ on γ. Arguing on part of Σ itself, by the convex hull property, we see that there are m_0 components of $\gamma \cap \{x_1 \geq R_2/(2\,\Omega_1)\}$ which are in distinct components of $\Sigma \cap \{x_1 \geq R_2/(2\,\Omega_1)\}$. Hence, see Figure 15, there are m_0 distinct $y_i \in \gamma$ and (nodal) curves

$$\sigma_0, \ldots, \sigma_{m_0-1} \subset \{x_1 = R_2/\Omega_1\} \cap \Sigma$$

with $\partial\sigma_i = \{y_i, z_i\}$, $\sigma_i \cap \gamma = \{y_i\}$, $z_i \in \partial\Sigma \cap \{x_1 = R_2/\Omega_1\} \subset \partial B_{R_0}$, and for $i \neq j$

$$\operatorname{dist}_\Sigma(\sigma_i, \sigma_j) > R_2/\Omega_1\,. \tag{II.3.3}$$

Order the σ_i's using the ordering of the y_i's in γ and set $i_1 = 0$, $i_2 = 8\,\Omega_1^2\,\omega + 16\,m_1$, $i_3 = 16\,\Omega_1^2\,\omega + 16\,m_1 + m$, and $i_4 = m_0 - 1$. Let $\gamma_1, \gamma_2, \gamma_3 \subset \gamma$ be the curves

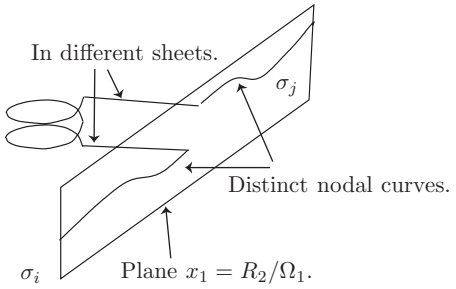

Figure 15: The proof of Corollary II.3.1: The nodal curves.

- from $y_{4\,\Omega_1^2\,\omega}$ to $y_{4\,\Omega_1^2\,\omega+16\,m_1}$,
- from $y_{12\,\Omega_1^2\,\omega+16\,m_1}$ to $y_{12\,\Omega_1^2\,\omega+16\,m_1+m}$,
- from $y_{20\,\Omega_1^2\,\omega+16\,m_1+m}$ to $y_{20\,\Omega_1^2\,\omega+32\,m_1+m}$.

Hence, $\gamma_1, \gamma_2, \gamma_3 \subset \gamma$ are $16\,m_1$-, m-, $16\,m_1$-valued graphs, respectively, with γ_2 centered on Σ^M, each γ_j between y_{i_j} and $y_{i_{j+1}}$, and for $j = 1, 2, 3$

$$\min_{\{k\,|\,y_k \in \gamma_j\}} \{|i_j - k|, |i_{j+1} - k|\} \geq 4\,\Omega_1^2\,\omega\,. \tag{II.3.4}$$

Next, we construct the curves γ_j^∂ needed to apply Corollary II.1.23 to each γ_j. We will also use (II.3.3) and (II.3.4) to separate the γ_j's. For $k_1 < k_2$, let $\gamma(k_1, k_2) \subset \Sigma$ be the union of σ_{k_1}, σ_{k_2}, and the curve in γ from y_{k_1} to y_{k_2}. Since Σ is a disk, $\partial\gamma(k_1, k_2) \subset \partial\Sigma$, and $\partial\Sigma \setminus \partial B_{R_0}$ is connected, one component $\Sigma(k_1, k_2)$ of $\Sigma \setminus \gamma(k_1, k_2)$ has $\partial\Sigma(k_1, k_2) \cap \partial\Sigma \subset \partial B_{R_0}$. By the fact that the σ_i's do not cross η, it is easy to see that $\mathbf{n}_\gamma$ points into $\Sigma(k_1, k_2)$ and

$$\Sigma(j_1, j_2) \cap \Sigma(k_1, k_2) = \Sigma(\max\{j_1, k_1\}, \min\{j_2, k_2\})\,, \tag{II.3.5}$$

where, by convention, $\Sigma(k_1, k_2) = \emptyset$ if $k_1 > k_2$. Set $\gamma_j^\partial = \gamma(i_j, i_{j+1})$ and note that $\gamma_j \subset \gamma_j^\partial$ and $\partial\gamma_j^\partial \subset \partial\Sigma$. Set $S_j = S_{\Omega_1\,\omega\,R_2}(\gamma_j)$. By (II.3.4) and (II.3.5), any curve $\tilde{\eta} \subset \Sigma(i_j, i_{j+1})$ from γ_j to $\gamma_j^\partial \setminus (\gamma \cup \partial B_{R_0})$ hits at least $4\,\Omega_1^2\,\omega$ of the σ_i's and so, by (II.3.3), $\text{Length}(\tilde{\eta}) > 2\,\Omega_1\,\omega\,R_2$. Combining this with $R_0 > 4\Omega_1\,\omega\,R_2$, we get

$$\text{dist}_{\Sigma(i_j, i_{j+1})}(\gamma_j, \partial\Sigma(i_j, i_{j+1}) \setminus \gamma_j) > 2\,\Omega_1\,\omega\,R_2\,. \tag{II.3.6}$$

Fix $x \in \gamma_j$ and γ_x (the geodesic normal to γ_j at x and of length $\Omega_1\,\omega\,R_2$). By (II.0.23), the first point (after x) where γ_x hits $\partial\Sigma(i_j, i_{j+1})$ cannot be in γ. Consequently, (II.3.6) implies that $\gamma_x \subset \Sigma(i_j, i_{j+1})$ and so $\gamma_x \cap \gamma_j^\partial = \{x\}$ and γ_j^∂ separates S_j from $S_k \cup \mathcal{T}_{R_2/(2\,\Omega_1)}(\partial\Sigma)$ for $j \neq k$.

The rest of the proof (see Figure 16) is to sandwich Σ^M between two graphs that will be given by Corollary II.1.23 and then deduce from stability that Σ^M itself extends to a graph. Namely, applying Corollary II.1.23 to

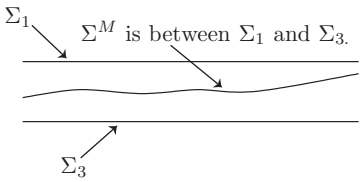

Figure 16: The proof of Corollary II.3.1: Sandwiching between two graphical pieces.

γ_1, γ_3 (with $r_1 = R_2/\Omega_1$), we get 2-valued graphs $\Sigma_{d,1} \subset S_1$, $\Sigma_{d,3} \subset S_3$ over $B_{2\,\omega\,R_2} \cap P_i \setminus B_{R_2/2}$ $(i = 1, 3)$ with $|A| \leq \varepsilon/(2\,r)$ and gradient $\leq \varepsilon/2 \leq 1/8$. Here P_i is a plane through 0. Using $|A| \leq \varepsilon/(2\,r)$ and $\text{dist}_{S_i}(\gamma, \Sigma_{d,i}) < 2\,R_2$, we see easily that $\Sigma_{d,i} \cap \Sigma_g \neq \emptyset$. Hence, $\Sigma_{d,i}$ contains a 3/2-valued graph Σ_i over $D_{3\,\omega\,R_2/2} \setminus D_{2\,R_2/3}$ with

$$\text{gradient } \leq \tan\left(\tan^{-1}(1/4) + 2\tan^{-1}(1/8)\right) < 3/4\,.$$

By construction, Σ^M is pinched between Σ_1 and Σ_3 which are graphs over each other with separation $\leq \omega^C\,\delta\,R_2$ (by the Harnack inequality). Since Σ is stable, it follows that if δ is small, then Σ^M extends to an m-valued graph Σ_2 over $D_{5\,\omega\,R_2/4} \setminus D_{4\,R_2/5}$ with Σ_2 between Σ_1 and Σ_3. In particular, Σ_2 is a graph over Σ_1. Finally, since Σ_1 is a graph with gradient $\leq 3/4$ and $|A| \leq \varepsilon/(2\,r)$, we get that Σ_2 is a graph with gradient ≤ 1 and $|A| \leq \varepsilon/r$ (cf. Lemma I.0.9). □

Combining this and Proposition II.2.12, Σ^M extends with separation growing sublinearly:

COROLLARY II.3.7. *Given $1/4 \geq \varepsilon > 0$, there exist $\Omega_0, m_0, \delta_0 > 0$ so that for any r_0, r_2, R_2, R_0 with $\Omega_0\,r_0 \leq \Omega_0\,r_2 < R_2 < R_0/\Omega_0$ the following holds*:

Let $\Sigma_g \subset \Sigma$ be an m_0-valued graph over $D_{R_2} \setminus D_{r_2}$ with gradient $\leq \tau_1 \leq \tau_k$, separations between the top and bottom sheets of $\Sigma^M (\subset \Sigma_g)$ and Σ_g are $\leq \delta_1\,R_2$ and $\leq \delta_0\,R_2$, respectively, over ∂D_{R_2}, and

$$\Pi^{-1}(D_{r_2}) \cap \Sigma_g \subset \{|x_3| \leq r_2/2\}\,.$$

If a curve $\eta \subset \Pi^{-1}(D_{r_2}) \cap \Sigma \setminus \partial B_{R_0}$ connects Σ_g to

$$\partial\Sigma \setminus \partial B_{R_0}\,,$$

then Σ^M extends as a graph over $D_{2\,R_2} \setminus D_{r_2}$ with gradient $\leq \tau_1 + 3\,\varepsilon$, $|A| \leq \varepsilon/r$ over $D_{2\,R_2} \setminus D_{R_2}$, and, for $R_2 \leq s \leq 2\,R_2$, separation $\leq (s/R_2)^{1/2}\,\delta_1\,R_2$ over $D_s \setminus D_{R_2}$.

Proof. Let $\delta_p > 0, N_g > 5$ be given by Proposition II.2.12 with $\alpha = 1/2$. Let $\Omega_1, m_0, \delta > 0$ be given by Corollary II.3.1 with $m = N_g + 3$ and $\omega = 2\,\mathrm{e}^{N_g}$. We will set $\delta_0 = \delta_0(\delta, \delta_p, N_g)$ with $\delta > \delta_0 > 0$ and $\Omega_0 = 4\,\Omega_1\,\mathrm{e}^{N_g}$.

By Corollary II.3.1, Σ^M extends to a graph

$$\Sigma^{-(N_g+3)\pi,(N_g+3)\pi}_{r_2,2\,\mathrm{e}^{N_g}\,R_2}$$

of a function v with $|\nabla v| \leq 1$ and $|A| \leq \varepsilon/r$ over $D_{2\,\mathrm{e}^{N_g}\,R_2} \setminus D_{R_2}$. Integrating

$$|\nabla |\nabla v|| \leq |A|\,(1+|\nabla v|^2)^{3/2} \leq 2^{3/2}\,\varepsilon/r\,,$$

we get that $|\nabla v| \leq \tau_1 + 4\,\varepsilon\,\log 2 \leq \tau_1 + 3\,\varepsilon$ on $D_{2R_2} \setminus D_{R_2}$.

For $\delta_0 = \delta_0(N_g, \delta_p) > 0$, writing Σ as a graph over itself and using the Harnack inequality, we get a solution $0 < u < \delta_p\,R_2$ of the minimal graph equation on an N_g-valued graph over $D_{\mathrm{e}^{N_g}\,R_2} \setminus D_{\mathrm{e}^{-N_g}\,R_2}$. Applying Proposition II.2.12 to u gives the last claim. □

The next lemma uses the Harnack inequality to show that if Σ^M extends with small separation, then so do the other sheets. The only complication is to keep track of $\partial\Sigma$.

LEMMA II.3.8. *Given $N \in \mathbf{Z}_+$, there exist $C_3, \delta_2 > 0$ so that for $r_0 \leq s < R_0/8$ the following holds*:

Let $\Sigma_g \subset \Sigma \cap \{|x_3| \leq 2\,s\}$ be an N-valued graph over $D_{2\,s} \setminus D_s$. If a curve $\eta \subset \Pi^{-1}(D_s) \cap \Sigma \setminus \partial B_{R_0}$ connects Σ_g to $\partial\Sigma \setminus \partial B_{R_0}$, and Σ^M extends graphically over $D_{4\,s} \setminus D_s$ with gradient $\leq \tau_2 \leq 1$ and separation

$$\leq \delta_3\,s \leq \delta_2\,s\,,$$

then Σ_g extends to an N-valued graph over $D_{3\,s} \setminus D_s$ with gradient $\leq \tau_2 + C_3\,\delta_3$ and separation between the top and bottom sheets $\leq C_3\,\delta_3\,s$.

Proof. Suppose N is odd (the even case is virtually identical). Fix $y_{-N}, \ldots, y_N \in \Sigma_g$ with y_j over $\{\rho = 2\,s,\, \theta = j\,\pi\}$. Let $\gamma_0, \gamma_2 \subset \Sigma^M$ be the graphs over $\{2s \leq \rho \leq 3s, \theta = 0\}$ and $\{2s \leq \rho \leq 3s, \theta = 2\,\pi\}$, respectively, with $\partial\gamma_0 = \{y_0, z_0\}$ and $\partial\gamma_2 = \{y_2, z_2\}$.

As in the proof of Corollary II.3.1, there are nodal curves

$$\sigma_{-N}, \ldots, \sigma_N \subset \{x_1 = -2\,s\} \cap \Sigma$$

from y_j (for j odd) to ∂B_{R_0} so that

(1) Any curve in $\Sigma \setminus \Pi^{-1}(\partial D_{2\,s})$ from z_0 to $\partial\Sigma \setminus \partial B_{R_0}$ hits either every σ_j with $j > 0$ or every σ_j with $j < 0$.

(2) For $i < j$, σ_i and σ_j do not connect in $\Pi^{-1}(D_{4s}) \cap \{x_1 \leq -2\,s\} \cap \Sigma$.

(3) $\mathrm{dist}(\cup_j \sigma_j, \partial\Sigma \setminus \partial B_{R_0}) \geq s$.

Note that (2) follows easily from the convex hull property when $i \neq -N$ or $j \neq N$; the case $i = -N$ and $j = N$ follows since Σ separates y_{-N}, y_N in $\Pi^{-1}(D_{4s}) \cap \{x_1 \leq -2\,s\}$.

By the curvature estimate for stable surfaces of [Sc] and the Harnack inequality for the minimal graph equation, there exist $C_4, \delta_4 > 0$ so that if $z_3, z_4 \in \Sigma \setminus \mathcal{T}_{s/4}(\partial\Sigma)$, $\Pi(z_3) = \Pi(z_4)$, and

$$0 < |z_3 - z_4| \leq \delta_5\, s \leq \delta_4\, s\,,$$

then $\mathcal{B}_{s/8}(z_4)$ is a graph over (a subset of) $\mathcal{B}_{s/7}(z_3)$ of a function $u > 0$ with

$$|\nabla u| \leq \min\{1/2, C_4\,\delta_5\}\,.$$

The lemma now follows easily by repeatedly applying this and using (1)–(3) to stay away from $\partial\Sigma$ until we have recovered all N sheets. □

II.4. Proof of Theorem II.0.21

Let again $\Sigma \subset B_{R_0}$ be a stable embedded disk with

$$\partial\Sigma \subset B_{r_0} \cup \partial B_{R_0} \cup \{x_1 = 0\}$$

and $\partial\Sigma \setminus \partial B_{R_0}$ connected. We will use the notation of (II.2.5), so that $\Sigma^{0,2\pi}_{r_3,r_4}$ is an annulus with a slit as defined in [CM3]. The next lemma is an easy consequence of Theorem 3.36 of [CM3].

LEMMA II.4.1. *Given $\tau_0 > 0$, there exists $0 < \varepsilon_1 = \varepsilon_1(\tau_0) < 1/24$ so that the following holds*:

If $2r_0 \leq 1 < r_3 \leq R_0/2$ and $\Sigma^{0,2\pi}_{1,r_3} \subset \Sigma$ is the graph of a function u with $|\nabla u| \leq 1/12$, $\max_{\Sigma^{0,2\pi}_{1,1}}(|u| + |\nabla u|) \leq 2\,\varepsilon_1$, $|A| \leq \varepsilon_1/r$, and for $1 \leq t \leq r_3$ the separation over ∂D_t is

$$\leq 4\,\pi\,\varepsilon_1\,t^{1/2}\,,$$

then $|\nabla u| \leq \tau_0$.

Lemma II.4.1 follows from Theorem 3.36 of [CM3] and two facts:

- Since Σ is a graph over a larger set in $\mathcal{P}$ (by stability and the fact that $\partial\Sigma \subset B_{r_0} \cup \partial B_{R_0} \cup \{x_1 = 0\}$), the bound for the separation and estimates for the minimal graph equation over Σ give a bound for the difference in the two values of ∇u along the slit (cf. Proposition II.2.12).

- Theorem 3.36 of [CM3] actually applies directly to $B_{3r_3/4} \cap \Sigma^{0,2\pi}_{1,r_3} \setminus B_2$ to get $|\nabla u| \leq \tau_0/2$ on $D_{r_3/2} \setminus D_2$; integrating

  $$|\nabla|\nabla u|| \leq |A|\,(1 + |\nabla u|^2)^{3/2} \leq 2\,\varepsilon_1/r$$

  then gives $|\nabla u| \leq \tau_0$ on $D_{r_3} \setminus D_1$.

We will prove Theorem II.0.21 by repeatedly applying Corollary II.3.7 to extend Σ^M as a graph, Lemma II.4.1 to get an improved gradient bound, and then Lemma II.3.8 to extend additional sheets.

Proof of Theorem II.0.21. Set $\tau_0 = \min\{\tau, \tau_k, 1/24\}/2$ and let $\varepsilon_1 = \varepsilon_1(\tau_0)$ with

$$0 < \varepsilon_1 < 1/72$$

be given by Lemma II.4.1. The constants Ω_0, m_0, δ_0 are given by Corollary II.3.7 (depending on ε_1) and $C_3, \delta_2 > 0$ are from Lemma II.3.8 with $N = m_0$. Set $N_1 = m_0$, $\Omega_1 = 2\,\Omega_0$, and choose $\varepsilon > 0$ so the following three properties hold:

$$\varepsilon < \min\{\frac{\varepsilon_1}{2},\, \frac{\tau_0}{4\,\pi\,2^{1/2}\,C_3},\, \frac{\delta_0}{2\,\pi\,2^{1/2}\,C_3},\, \frac{\delta_0}{2\,\pi\,m_0},\, \frac{\delta_2}{4\,\pi\,2^{1/2}}\}\,, \tag{II.4.2}$$

$$\Pi^{-1}(D_{r_0}) \cap \Sigma_g \subset \{|x_3| \leq r_0/2\}\,,$$

$$|A| \leq \varepsilon_1/r \text{ on } \Sigma^M \setminus B_{2\,r_0}\,.$$

To arrange the last condition, we use the gradient bound, stability, and second derivative estimates for the minimal graph equation (in terms of the gradient bound). Note that, integrating the bound gradient $\leq \varepsilon$ around the circle ∂D_t, we get that the separation between the top and bottom sheets of $\Sigma^{0,2\pi}_{r_0,1}$ and $\Sigma^{-m_0\pi,m_0\pi}_{r_0,1}$ over ∂D_t are at most $2\,\pi\,\varepsilon\,t$ and $2\,\pi\,m_0\,\varepsilon\,t$, respectively. Note also that $\Pi^{-1}(D_{3\,r_0}) \cap \Sigma_g \subset \{|x_3| \leq 3\,\varepsilon\,r_0\}$.

(1) Apply Corollary II.3.7 (with $r_2 = r_0, R_2 = 1, \tau_1 = 2\,\tau_0$) to extend $\Sigma^{0,2\pi}_{r_0,1}$ to a graph $\Sigma^{0,2\pi}_{r_0,2}$ with gradient $\leq 2\,\tau_0 + 3\,\varepsilon_1 < 1/12$, $|A| \leq \varepsilon_1/r$ over $D_2 \setminus D_1$, and, for $1 \leq t \leq 2$,

$$\text{separation } \leq 2\,\pi\varepsilon\,t^{1/2} \text{ over } \partial D_t\,. \tag{II.4.3}$$

(2) By Lemma II.4.1 (with $r_3 = 2$), $\Sigma^{0,2\pi}_{1,2}$ and hence $\Sigma^{0,2\pi}_{r_0,2}$ have gradient $\leq \tau_0$.

(3) By Lemma II.3.8 (with $N = m_0, s = 1/2, \tau_2 = \tau_0, \delta_3 = 4\,\pi\varepsilon\,2^{1/2}$), $\Sigma^{0,2\pi}_{r_0,3/2}$ is contained in an m_0-valued graph $\Sigma^{-m_0\pi,m_0\pi}_{r_0,3/2} \subset \Sigma$ over $D_{3/2} \setminus D_{r_0}$ with gradient $\leq \tau_0 + C_3\,4\,\pi\varepsilon\,2^{1/2} < 2\,\tau_0$ and separation $\leq C_3\,2\,\pi\varepsilon\,2^{1/2} < \delta_0$.

Repeat (1)–(3) with: (1) $R_2 = 3/2$ to extend $\Sigma^{0,2\pi}_{r_0,3/2}$ to $\Sigma^{0,2\pi}_{r_0,3}$ with (II.4.3) holding for $1 \leq t \leq 3$, (2) $r_3 = 3$ so that $\Sigma^{0,2\pi}_{r_0,3}$ has gradient $\leq \tau_0$, (3) $s = 3/2$ to get $\Sigma^{-m_0\pi,m_0\pi}_{r_0,9/2} \subset \Sigma$, and then again (1) $R_2 = 9/2$, etc., giving the theorem. □

Part III. The general case of Theorem I.0.8

III.1. Constructing multi-valued graphs in disks in slabs

Using Part I, we show next that an embedded minimal disk in a slab contains a multi-valued graph if it is not a graph. We can therefore apply Part II to get almost flatness of a corresponding stable disk past the slab. This is needed when the minimal surface is not in a thin slab.

PROPOSITION III.1.1. *There exists $\beta > 0$ so that the following holds:*
Let $\Sigma^2 \subset B_{r_0} \cap \{|x_3| \leq \beta\, h\}$ be an embedded minimal disk with $\partial\Sigma \subset \partial B_{r_0}$. If a component Σ_1 of $B_{10\,h} \cap \Sigma$ is not a graph, then Σ contains an N-valued graph over $D_{r_0-2\,h} \setminus D_{(60+20\,N)\,h}$.

Proof. The proof has four steps. First we show, by using Lemma I.0.11 twice, that over a truncated sector in the plane, i.e., over

$$S_{s_1,s_2}(\theta_1,\theta_2) = \{(\rho,\theta) \,|\, s_1 \leq \rho \leq s_2,\, \theta_1 \leq \theta \leq \theta_2\}\,, \tag{III.1.2}$$

we have three distinct components of Σ. Second, we separate these by stable disks and order them by height. Third, we use Proposition I.0.16 to show that the "middle" component is a graph over a large sector. Fourth, we repeatedly use the appendix to extend the top and bottom components around the annulus and then Proposition I.0.16 to extend the middle component as a graph. This will give the desired multi-valued graph.

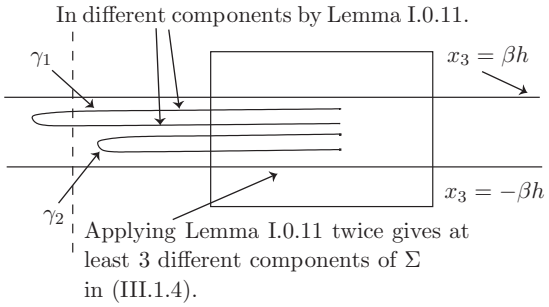

Figure 17: Proof of Proposition III.1.1:
Step 1: Finding the three components.

For $j = 1$ and 2, let Σ_j be the component of $B_{20\,j\,h} \cap \Sigma$ containing Σ_1. By the maximum principle, each Σ_j is a disk. Rado's theorem (see, e.g., [CM1]) gives points

$$z_j \in \Pi^{-1}(\partial D_{(20\,j-10)\,h}) \cap \Sigma_j\,,$$

for $j = 1, 2$, where Σ is not graphical. Rotate $\mathbf{R}^2$ so that $z_1, z_2 \in \{x_1 \geq 0\}$ and set $z = (r_0, 0, 0)$. Apply Lemma I.0.11 twice as in the first step of the proof of Proposition I.0.16 to get (see Figure 17):

(1) Disjoint curves $\gamma_1, \gamma_2 \subset \Sigma$ with $\partial\gamma_k \subset \partial B_{r_0/2}$,

$$\gamma_k \subset B_{5\,h}(z_k) \cup T_h(\partial D_{(20\,k-10)\,h} \cap \{x_1 \geq 0\}) \cup T_h(\gamma_{0,z/2})\,, \tag{III.1.3}$$

which are $C\,\beta\,h$-almost monotone in $T_h(\gamma_{0,z/2}) \setminus B_{20\,k\,h}$.

(2) For $k = 1, 2$ and $y_0 \in \gamma_{0,z/2} \setminus B_{20\,k\,h}$, there are components $\Sigma'_{y_0,k,1} \neq \Sigma'_{y_0,k,2}$ of $B_{5\,h}(y_0) \cap \Sigma$ each containing points of $B_h(y_0) \cap \gamma_k$.

It follows from (2) that, for $k = 1, 2$, there are components $\Sigma_{k,1}, \Sigma_{k,2}$ of

$$\Pi^{-1}(S_{42h,r_0-2\,h}(-3\pi/4, 3\pi/4)) \cap \Sigma$$

with $\Sigma'_{z/2,k,i} \subset \Sigma_{k,i}$. These components do not connect in

$$\Pi^{-1}(S_{40h,r_0}(-7\pi/8, 7\pi/8)) \cap \Sigma\,.$$

That is, Σ would otherwise contain a disk violating the maximum principle (as in the second step of Lemma I.0.11). The same argument gives $\Sigma_{i_1,i_1}, \Sigma_{i_2,i_2}, \Sigma_{i_3,i_3}$ which do not connect in

$$\Pi^{-1}(S_{40h,r_0}(-7\pi/8, 7\pi/8)) \cap \Sigma\,. \tag{III.1.4}$$

By the second step of Proposition I.0.16, if $\Sigma_{i,j}, \Sigma_{k,\ell}$ do not connect in

$$\Pi^{-1}(S_{40h,r_0}(-7\pi/8, 7\pi/8)) \cap \Sigma\,,$$

then there is a stable embedded disk Γ_α with $\partial\Gamma_\alpha \subset \Sigma$, $\Gamma_\alpha \cap \Sigma = \emptyset$, and a graph $\Gamma'_\alpha \subset \Gamma_\alpha$ over $S_{41h,r_0-h}(-13\pi/16, 13\pi/16)$ separating $\Sigma_{i,j}, \Sigma_{k,\ell}$. Applying this twice (and reordering the k_ℓ, i_ℓ), we get $\Gamma'_1 \subset \Gamma_1$ and $\Gamma'_2 \subset \Gamma_2$ so that each Σ_{k_ℓ,i_ℓ} is below Γ'_ℓ which is in turn below $\Sigma_{k_{\ell+1},i_{\ell+1}}$. Let γ_1^t and γ_1^b be top and bottom components of $\cup_j \gamma_j \setminus B_{40\,h}$ intersecting $\partial B_{r_0/2}$. Since $\Sigma_1 \subset \Sigma_2$, a curve $\gamma_1^m \subset B_{40\,h} \cap \Sigma$ connects γ_1^t to γ_1^b.

See Figure 18. By a slight variation of Proposition I.0.16 (with $\gamma = \gamma_1^t \cup \gamma_1^m \cup \gamma_1^b$), the middle component Σ_{k_2,i_2} is a graph over $S_{42\,h,r_0-2\,h}(-3\pi/4, 3\pi/4)$. This variation follows from steps one and three of that proof (step two there constructs barriers Γ_i which were constructed here above).

See Figure 19. Corollary A.10 gives curves

$$\gamma_2^t, \gamma_2^b \subset (B_{44\,h} \cup T_h(\gamma_{0,(0,r_0,0)}) \setminus \Pi^{-1}(D_{42\,h})) \cap \Sigma$$

from $\partial B_{43\,h} \cap \gamma_1^t$ and $\partial B_{43\,h} \cap \gamma_1^b$, respectively, to $\partial B_{r_0/2}$. In particular, γ_2^b is below Σ_{k_2,i_2} and γ_2^t is above Σ_{k_2,i_2}; i.e., Σ_{k_2,i_2} is still a middle component. Again by the maximum principle, this gives 3 distinct components of

$$\Pi^{-1}(S_{46\,h,r_0-2\,h}(-\pi/4, 5\pi/4)) \cap \Sigma$$

which do not connect in

$$\Pi^{-1}(S_{45\,h,r_0}(-3\pi/8, 11\pi/8)) \cap \Sigma\,.$$

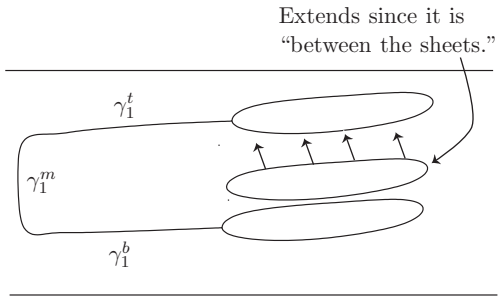

Figure 18: Proof of Proposition III.1.1:
Step 3: Extending the middle component as a graph.

By Proposition I.0.16, Σ_{k_2,i_2} further extends as a graph over $S_{46\,h,r_0-2\,h}(-\pi/4,5\pi/4)$, giving a graph $\Sigma^{-3\pi/4,5\pi/4}_{46\,h,r_0-2\,h}$ over $S_{46\,h,r_0-2\,h}(-3\pi/4,5\pi/4)$. By Rado's theorem, this graph cannot close up. Repeating this with

$$\gamma_3^t,\gamma_3^b \subset (B_{49\,h}\cup T_h(\gamma_{0,(-r_0,0,0)})\setminus \Pi^{-1}(D_{47\,h}))\cap\Sigma\,,$$

etc., eventually gives the proposition. □

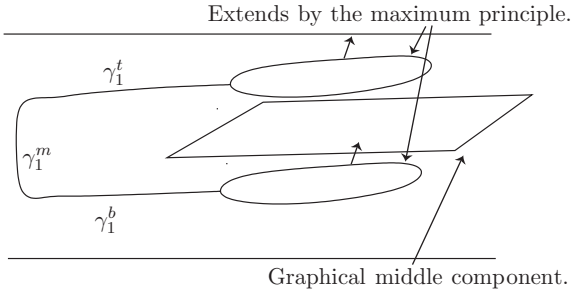

Figure 19: Proof of Proposition III.1.1:
Step 4: Extending the top and bottom components by the maximum principle. They stay disjoint since the middle component is a graph separating them.

III.2. Proof of Theorem I.0.8

In this section, we generalize Proposition I.0.16 to when the minimal surface is not in a slab; i.e., we show Theorem I.0.8. $\Sigma^2\subset B_{c_1\,r_0}\subset\mathbf{R}^3$ will be an embedded minimal disk, $\partial\Sigma\subset\partial B_{c_1\,r_0}$, $c_1\geq 4$, and $y\in\partial B_{2\,r_0}$. $\Sigma_1,\Sigma_2,\Sigma_3$ will be distinct components of $B_{r_0}(y)\cap\Sigma$.

Lemma III.2.1. *Given $\bar\beta>0$, there exist $2\,c_2<c_4<c_3\leq 1$ so that the following holds*:

Let Σ'_3 be a component of $B_{c_3\,r_0}(y)\cap\Sigma_3$ and $y_i \in B_{c_2\,r_0}(y)\cap\Sigma_i$ for $i=1,2$. If y_1, y_2 are in distinct components of

$$B_{c_4\,r_0}(y)\setminus\Sigma'_3\,,$$

then there are disjoint stable embedded minimal disks $\Gamma_1,\Gamma_2\subset B_{r_0}(y)\setminus\Sigma$ with $\partial\Gamma_i=\partial\Sigma_i$, and (after a rotation) graphs $\Gamma'_i\subset\Gamma_i$ over $D_{3\,c_3\,r_0}(y)$ so that y_1, y_2, Σ'_3 are each in their own component of

$$\Pi^{-1}(D_{3\,c_3\,r_0}(y))\setminus(\Gamma'_1\cup\Gamma'_2)$$

and $\Gamma'_1,\Gamma'_2\subset\{|x_3-x_3(y)|\leq\bar\beta\,c_3\,r_0\}$.

Proof. This follows exactly as in the second step of the proof of Proposition I.0.16. □

Proof of Theorem I.0.8. Let $N_1,\Omega_1,\varepsilon>0$ be given by Theorem II.0.21 (with $\tau=1$). Assume that N_1 is even. Let $\beta>0$ be from Proposition III.1.1. Set

$$\bar\beta=\min\left\{\beta_s,\,\varepsilon,\,\varepsilon/C_g,\,\beta/(6\,[60+20\,(N_1+3)])\right\}/(5\,\Omega_1)\,, \tag{III.2.2}$$

where β_s, C_g are as in Lemma I.0.9. Let c_2, c_3, c_4 and $\Gamma'_i\subset\Gamma_i$ be given by Lemma III.2.1. Set

$$c_5=(60+20\,(N_1+3))\bar\beta\,c_3/\beta\,,$$

so that $c_5\leq c_3/(30\,\Omega_1)$. Finally, set $c_1=16\,\Omega_1$.

We will suppose that Σ'_3 is not a graph at $z'\in\Sigma'_3$ and deduce a contradiction. Set $z=\Pi(z')$. Since Σ'_3 separates y_1, y_2, it is in the slab between Γ'_1,Γ'_2. By Proposition III.1.1 (with $h=\bar\beta\,c_3\,r_0/\beta$) and (III.2.2), Σ contains an (N_1+3)-valued graph Σ_g over $D_{c_3\,r_0}(z)\setminus D_{c_5\,r_0}(z)$ and Σ_g is also in the slab. Let $\sigma_g\subset\Sigma_g$ be the (N_1+2)-valued graph over $\partial D_{c_5\,r_0}(z)$ (see Figure 20). Let E be the region in

$$\Pi^{-1}(D_{c_3\,r_0/2}(z)\setminus D_{c_3\,r_0/(2\,\Omega_1)}(z))$$

between the sheets of the (concentric) (N_1+1)-valued subgraph of Σ_g.

The first step is to find a curve $\gamma_3\subset\Sigma$ containing σ_g so that any stable disk with boundary γ_3 is forced to spiral. Also, γ_3 will have six pieces: σ_g, two segments, γ^t,γ^b, in Σ_g which are graphs over a portion of the $\{x_1>x_1(z)\}$ part of the x_1-axis, two nodal curves, σ^t,σ^b, in $\{x_1=\text{constant}\}$, and a segment σ^∂ in $\partial\Sigma$. Since Σ_g is a graph, there are graphs $\gamma^t,\gamma^b\subset\Sigma_g$ over a portion of the $\{x_1>x_1(z)\}$ part of the x_1-axis from $\partial\sigma_g$ to

$$y^t, y^b\in\{x_1=x_1(z)+3\,c_5\,r_0\}\cap\Sigma\,.$$

By the maximum principle (as in the proof of Corollary II.3.1), there are nodal curves

$$\sigma^t,\sigma^b\subset\{x_1=x_1(z)+3\,c_5\,r_0\}\cap\Sigma$$

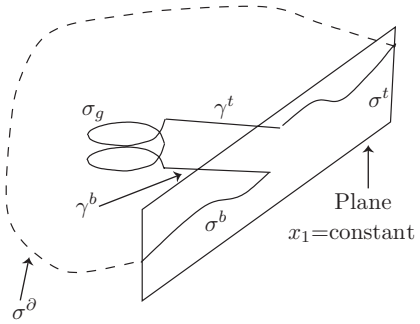

Figure 20: The curve γ_3 in the proof of Theorem I.0.8. ($\gamma_3 = \sigma^b \cup \gamma^b \cup \sigma_g \cup \gamma^t \cup \sigma^t \cup \sigma^\partial$.)

from y^t, y^b, respectively, to $y_0^t, y_0^b \in \partial\Sigma$. Finally, connect y_0^t, y_0^b by a curve $\sigma^\partial \subset \partial\Sigma$ and set

$$\gamma_3 = \sigma^b \cup \gamma^b \cup \sigma_g \cup \gamma^t \cup \sigma^t \cup \sigma^\partial \, .$$

By [MeYa], there is a stable embedded disk $\Gamma \subset B_{c_1 r_0} \setminus \Sigma$ with $\partial\Gamma = \gamma_3$. Note that $\partial\Gamma \setminus \partial B_{r_0}$ is connected.

We claim that σ^t, σ^b do not intersect between any two of the components $\{\sigma_i\}$ of

$$B_{(c_3 - 2c_5)\, r_0}(z) \cap \{x_1 = x_1(z) + 3\, c_5\, r_0\} \cap \Sigma_g \, .$$

If not, we can assume that a curve $\sigma \subset \sigma^t$ connects y^t to a point y_0 between σ_i, σ_{i+1}. By (a slight variation of) Proposition I.0.16, the portion Σ_{y_0} of Σ between the i-th and $(i+1)$-st sheets of

$$B_{(c_3 - c_5)\, r_0}(z) \cap \Sigma_g \setminus \Pi^{-1}(D_{2\, c_5\, r_0}(z))$$

is a graph (in fact, "all the way around"). Note that $B_{3\, c_5\, r_0}(z) \cap \Sigma_{y_0}$ and $B_{3\, c_5\, r_0}(z) \cap \Sigma_g$ are in the same component of $B_{3\, c_5\, r_0}(z) \cap \Sigma$, since otherwise the stable disk between them given by [MeYa] would, by Lemma I.0.9, intersect Σ_g. We can therefore apply the maximum principle as in the proof of Corollary II.3.1 (i.e., the case $y_0 \in \sigma_j$ for some j) to get the desired contradiction.

We will show next that Γ contains an N_1-valued graph Γ_g over $D_{c_3 r_0/2}(z) \setminus D_{c_3 r_0/(2\,\Omega_1)}(z)$ with gradient $\leq \varepsilon$,

$$\Pi^{-1}(D_{c_3 r_0/(2\,\Omega_1)}(z)) \cap (\Gamma_g)^M \subset \{|x_3 - x_3(z)| \leq \varepsilon\, c_3\, r_0/(2\,\Omega_1)\} \, ,$$

and a curve $\eta \subset \Pi^{-1}(D_{c_3 r_0/(2\,\Omega_1)}(z)) \cap \Gamma \setminus \partial B_{r_0}$ connects Γ_g to $\partial\Gamma \setminus \partial B_{r_0}$. By the previous paragraph,

$$\text{dist}_\Gamma(E \cap \Gamma, \partial\Gamma) > c_3\, r_0/(5\,\Omega_1) \, . \tag{III.2.3}$$

By (the proof of) Lemma I.0.9 (with $h = c_3\, r_0/(5\,\Omega_1)$ and $\beta = 5\,\Omega_1\,\bar{\beta}$), (III.2.2), and (III.2.3), we have that each component of $E \cap \Gamma$ is a multi-valued graph

with

$$\text{gradient } \leq 5\, C_g\, \Omega_1\, \bar{\beta} \leq \varepsilon\,.$$

Let $\sigma_c \subset E$ be a graph over $\partial D_{c_3\, r_0/(2\,\Omega_1)}(z)$. Since σ_c separates

$$\Pi^{-1}(\partial D_{c_3\, r_0/(2\,\Omega_1)}(z)) \cap \gamma^t \text{ and } \Pi^{-1}(\partial D_{c_3\, r_0/(2\,\Omega_1)}(z)) \cap \gamma^b$$

in the cylinder $\Pi^{-1}(\partial D_{c_3\, r_0/(2\,\Omega_1)}(z))$ (and the description of $\partial\Gamma$), there is a curve

$$\eta \subset \Pi^{-1}(D_{c_3\, r_0/(2\,\Omega_1)}(z)) \cap \Gamma \setminus \partial B_{r_0}$$

from $\Gamma \cap \sigma_c$ to $\partial\Gamma \setminus \partial B_{r_0}$. Hence, since E is between the sheets of an (N_1+1)-valued graph, we get the desired Γ_g.

Combining all of this, Theorem II.0.21 gives a 2-valued graph $\Gamma_d \subset \Gamma$ over

$$D_{c_1\, r_0/(2\,\Omega_1)}(z) \setminus D_{c_3\, r_0/(2\,\Omega_1)}(z)$$

with gradient ≤ 1. Let $\hat{\gamma}$ be the component of $B_{(2-2\,c_3)\, r_0} \cap \gamma$ intersecting B_{r_0}. Note that since $\partial\gamma = \{y_1, y_2\}$ is separated by the slab between Γ_1', Γ_2' and $\gamma \setminus B_{r_0}$ is $c_2\, r_0$-almost monotone, Γ_d separates the endpoints of $\partial\hat{\gamma}$. Finally, as in the proof of Proposition I.0.16, we must have $\Gamma_d \cap \hat{\gamma} \neq \emptyset$. This contradiction completes the proof. □

Many variations of Theorem I.0.8 hold with almost the same proof. One of these is given in the following theorem:

THEOREM III.2.4. *There exist $d_1 \geq 8$ and $d_2 \leq 1$ so that the following holds*:

Let $\Sigma^2 \subset B_{d_1\, r_0} \subset \mathbf{R}^3$ be an embedded minimal disk with $\partial\Sigma \subset \partial B_{d_1\, r_0}$ and let $y \in \partial D_{5\, r_0}$. Suppose that $\Sigma_1, \Sigma_2 \subset \Sigma$ are disjoint graphs, over $D_{3r_0}(y)$ with gradient $\leq d_2$, which intersect $B_{d_2 r_0}(y)$. If

$$\Sigma_1 \text{ and } \Sigma_2 \text{ can be connected in } B_{3r_0} \cap \Sigma\,,$$

then any component of $B_{r_0}(y) \cap \Sigma$ which lies between them is a graph.

Part IV. Extending multi-valued graphs off the axis

In this section $\Sigma \subset B_{R_0} \subset \mathbf{R}^3$ will be an embedded minimal disk with $\partial\Sigma \subset \partial B_{R_0}$. In contrast to the results of Part II, Σ is no longer assumed to be stable.

Note that, by [Sc], we can choose $d_3 > 4$ so that: If $\Gamma_0 \subset B_{d_3\, s}$ with $\partial\Gamma_0 \subset \partial B_{d_3\, s}$ is stable, then each component of $B_{4\, s} \cap \Gamma_0$ is a graph (over some plane) with gradient $\leq 1/2$.

Proof of Theorem 0.3. The proof has two steps. First, the proofs of Theorem I.0.8 and Lemma II.3.8 give a stable disk $\Gamma \subset B_{R_0} \setminus \Sigma$ and a 4-valued graph $\Gamma_4 \subset \Gamma$ so that Σ^M "passes between" Γ_4. Second, (a slight variation of) Theorem III.2.4 gives the 2-valued graph $\Sigma_d \subset \Sigma$.

Before proceeding, we choose the constants. Let C_3, δ_2 be given by Lemma II.3.8 (with $N = 4$), d_1, d_2 be from Theorem III.2.4, and C_g, β_s be from Lemma I.0.9. Set

$$\tau_1 = \min\{\tau/(5\,C_g), \beta_s/5, d_2/10\}\,,$$
$$\tau_2 = \min\{\delta_2/3, \tau_1/(1+3\,C_3)\}\,.$$

Let $N_1, \Omega_1, \varepsilon$ be given by Theorem II.0.21 (with τ there equal to τ_2). For convenience, assume that $N_1 \geq 16$ is even, $\Omega_1 > 4$, and rename this ε as ε_1. Set $N = N_1 + 3$, $\Omega = \max\{d_1, 8\,d_3\,\Omega_1\}$, and

$$\varepsilon = \min\{\varepsilon_1, \varepsilon_1/(5\,C_g), \beta_s/5, 1/4, d_2/10\}\,. \tag{IV.0.5}$$

For $N_2 \leq N$ and $r_0 \leq r_2 < r_3 \leq 1$, let $E^{N_2}_{r_2,r_3}$ be the region in $\Pi^{-1}(D_{r_3} \setminus D_{r_2})$ between the sheets of the (concentric) N_2-valued subgraph of Σ_g. Note that

$$E^{N_2}_{r_2,r_3} \subset \{x_3^2 \leq \varepsilon^2\,(x_1^2 + x_2^2)\}\,.$$

As in the proof of Theorem I.0.8, let $\sigma_g \subset \Sigma_g$ be an (N_1+2)-valued graph over ∂D_{r_0} and let $\gamma_3 \subset \Sigma$ be a curve with six pieces: σ_g, two segments, γ^t, γ^b, in Σ_g which are graphs over a portion of the positive part of the x_1-axis, two nodal curves, σ^t, σ^b, in $\{x_1 = 2\,d_3\,r_0\}$, and $\sigma^\partial \subset \partial\Sigma$. By [MeYa], there is a stable embedded disk $\Gamma \subset B_{R_0} \setminus \Sigma$ with $\partial\Gamma = \gamma_3$.

Let $\{\sigma_i\}$ be the components of $B_{5/8} \cap \{x_1 = 2\,d_3\,r_0\} \cap \Sigma_g$ and suppose that a curve $\sigma \subset \sigma^t$ connects γ^t to a point y_0 between σ_i, σ_{i+1}. By Theorem III.2.4, the portion Σ_{y_0} with $y_0 \in \Sigma_{y_0}$ of $E^{N_1+5/2}_{3\,r_0,5/8} \cap \Sigma$ is a graph. Note that $B_{d_3\,r_0} \cap \Sigma_{y_0}$ and $B_{3\,r_0} \cap \Sigma_g$ are in the same component of $B_{d_3\,r_0} \cap \Sigma$, since otherwise the stable disk between them given by [MeYa] would intersect Σ_g (by [Sc]). Applying the maximum principle as before gives the desired contradiction. Hence, σ^t, σ^b do not intersect between any of the σ_i's. Therefore, if $z \in E^{N_1+1}_{4d_3\,r_0,1/2} \cap \Gamma$, then

$$\operatorname{dist}_\Gamma(z, \partial\Gamma) \geq |\Pi(z)|/4\,. \tag{IV.0.6}$$

By the same linking argument as before, $E^{N_1+1}_{4d_3\,r_0,1/2} \cap \Gamma$ contains an N_1-valued graph Γ_g over $D_{1/2} \setminus D_{4\,d_3\,r_0}$ with gradient $\leq 5\,C_g\,\varepsilon$,

$$\Pi^{-1}(\partial D_{4\,d_3\,r_0}) \cap \Gamma_g \subset \{|x_3| \leq 4\,\varepsilon\,d_3\,r_0\}\,,$$

and a curve

$$\eta \subset \Pi^{-1}(D_{4\,d_3\,r_0}) \cap \Gamma \setminus \partial B_{R_0}$$

connects Γ_g to $\partial\Gamma \setminus \partial B_{R_0}$. Since $\Omega_1 < 1/(8\,d_3\,r_0)$, Theorem II.0.21 implies that Γ contains a 2-valued graph Γ_d over $D_{R_0/\Omega_1} \setminus D_{4\,d_3\,r_0}$ with gradient $\leq \tau_2 < 1$. In particular,

$$\Gamma_d \subset \{x_3^2 \leq \tau_2^2(x_1^2 + x_2^2)\}\,.$$

Next, we apply Lemma II.3.8 to extend Γ_d to a 4-valued graph Γ_4 over $D_{5\,R_0/(6\,\Omega_1)} \setminus D_{5\,d_3\,r_0}$ with gradient $\leq \tau_2 + 3\,C_3\,\tau_2 \leq \tau_1$. Let E_Γ be the region in $\Pi^{-1}(D_{R_0/(2\,\Omega_1)} \setminus D_{15\,d_3\,r_0})$ between the sheets of the (concentric) 3-valued subgraph of Γ_4, so that $E_\Gamma \subset \{x_3^2 \leq \tau_1^2\,(x_1^2 + x_2^2)\}$.

If $z \in E_\Gamma \cap \Sigma$, then there is a curve $\gamma_z \subset \Gamma_4$ with each component of $\gamma_z \setminus \Pi^{-1}(D_{5\,d_3\,r_0})$ a graph over the segment $\gamma_{0,z}$, $\partial\gamma_z = \{y_z^2, y_z^4\}$, and y_z^2, y_z^4 are in distinct components of $B_{3\,|\Pi(z)|/5}(\Pi(z)) \cap \Gamma$ with z between these components. By (a slight variation of) Theorem III.2.4 (with $\Sigma \cup \Gamma$ as a barrier rather than just Σ), the portion of Σ inside $B_{R_0/d_1} \cap E_\Gamma$ is a graph over Γ_4. This is nonempty since $(\Sigma_g)^M$ begins in E_Γ, so we get the desired 2-valued graph Σ_d with gradient $\leq 5\,C_g\,\tau_1 \leq \tau$ (by Lemma I.0.9). □

Appendix A: Catenoid foliations

We recall here some consequences of the maximum principle for an embedded minimal surface Σ in a slab. Let $\mathrm{Cat}(y)$ be the vertical catenoid centered at $y = (y_1, y_2, y_3)$ given by

$$\mathrm{Cat}(y) = \{x \in \mathbf{R}^3 \mid \cosh^2(x_3 - y_3) = (x_1 - y_1)^2 + (x_2 - y_2)^2\}\,. \tag{A.1}$$

Given an angle $0 < \theta < \pi/2$, let $\partial N_\theta(y)$ be the cone

$$\{x \mid (x_3 - y_3)^2 = |x - y|^2\,\sin^2\theta\}\,. \tag{A.2}$$

Since $\cosh t > t$ for $t \geq 0$, it follows that $\partial N_{\pi/4}(y) \cap \mathrm{Cat}(y) = \emptyset$. Set

$$\theta_0 = \inf\{\theta \mid \partial N_\theta(y) \cap \mathrm{Cat}(y) = \emptyset\}\,, \tag{A.3}$$

so that $\partial N_{\theta_0}(y)$ and $\mathrm{Cat}(y)$ intersect tangentially in a pair of circles. Let $\mathrm{Cat}_0(y)$ be the component of $\mathrm{Cat}(y) \setminus \partial N_{\theta_0}(y)$ containing the neck

$$\{x \mid x_3 = y_3, (x_1 - y_1)^2 + (x_2 - y_2)^2 = 1\}\,.$$

If $x \in \mathrm{Cat}_0(y)$, then $\overline{y, x} \cap \mathrm{Cat}_0(y) = \{x\}$ since cosh is convex and $\cosh'(0) = 0$; i.e., $\mathrm{Cat}_0(y)$ is a radial graph. In particular, the dilations of $\mathrm{Cat}_0(y)$ about y are all disjoint and, consequently (see Figure 21), give a minimal foliation of the solid (open) cone

$$N_{\theta_0}(y) = \{x \mid (x_3 - y_3)^2 < |x - y|^2\,\sin^2\theta_0\}\,. \tag{A.4}$$

The leaves of this foliation have boundary in $\partial N_{\theta_0}(y)$ and are level sets of the function f_y given by

$$y + (x - y)/f_y(x) \in \mathrm{Cat}_0(y)\,. \tag{A.5}$$

Choose $\beta_A > 0$ small so that

$$\{x \mid |x_3 - y_3| \leq 2\,\beta_A\,h\} \setminus B_{h/8}(y) \subset N_{\theta_0}(y)$$

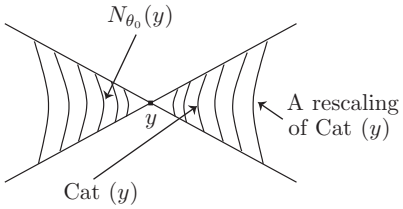

Figure 21: The catenoid foliation.

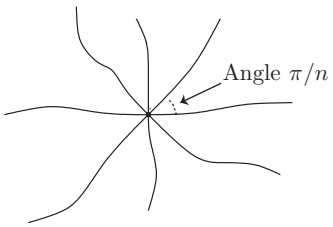

Figure 22: An n-prong singularity.

and

$$\{x \,|\, f_y(x) = 3\,h/16\} \cap \{x \,|\, |x_3 - y_3| \leq 2\,\beta_A\,h\} \subset B_{7\,h/32}(y)\,. \tag{A.6}$$

The intersection of two embedded minimal surfaces is locally given by $2n$ embedded arcs meeting at equal angles as in Figure 22, i.e., an "n-prong singularity" (e.g., the set where $(x+iy)^n$ is real); see Claim 1 in Lemma 4 of [HoMe]. This immediately implies the next lemma:

LEMMA A.7. *If $z \in \Sigma \subset N_{\theta_0}(y)$ is a nontrivial interior critical point of $f_y|_\Sigma$, then $\{x \in \Sigma \,|\, f_y(x) = f_y(z)\}$ has an n-prong singularity at z with $n \geq 2$.*

As a consequence, we get a version of the usual strong maximum principle:

LEMMA A.8. *If $\Sigma \subset N_{\theta_0}(y)$, then $f_y|_\Sigma$ has no nontrivial interior local extrema.*

In particular, we can use f_y to show that a minimal surface in a narrow slab either stays near its boundary or comes close to the center of the slab:

COROLLARY A.9. *If $\partial\Sigma \subset \partial B_h(y)$, $B_{3\,h/4}(y) \cap \Sigma \neq \emptyset$, and*

$$\Sigma \subset B_h(y) \cap \{x \,|\, |x_3 - y_3| \leq 2\,\beta_A\,h\}\,,$$

then $B_{h/4}(y) \cap \Sigma \neq \emptyset$.

Proof. Scaling (A.6) by 4, we get

$$\{x \in \Sigma \,|\, f_y(x) = 3\,h/4\} \subset B_{7\,h/8}(y) \setminus B_{3\,h/4}(y)\,.$$

By Lemma A.8, f_y has no interior minima in Σ so that the corollary now follows from

$$f_y(x) \leq |x - y|\,. \qquad \square$$

Iterating Corollary A.9 along a chain of balls gives the next corollary:

COROLLARY A.10. *If* $\Sigma \subset \{|x_3| \leq 2\,\beta_A\,h\}$, *points* $p, q \in \{x_3 = 0\}$ *satisfy* $T_h(\gamma_{p,q}) \cap \partial\Sigma = \emptyset$, *and*

$$y_p \in B_{h/4}(p) \cap \Sigma\,,$$

then a curve $\nu \subset T_h(\gamma_{p,q}) \cap \Sigma$ *connects* y_p *to* $B_{h/4}(q) \cap \Sigma$.

Proof. Choose points

$$y_0 = p, y_1, y_2, \ldots, y_n = q \in \gamma_{p,q}$$

with $|y_{i-1} - y_i| = h/2$ for $i < n$ and $|y_{n-1} - y_n| \leq h/2$. Repeatedly applying Corollary A.9 for $1 \leq i \leq n$, gives curves

$$\nu_i : [0,1] \to B_h(y_i) \cap \Sigma$$

with $\nu_1(0) = y_p$, $\nu_i(1) \in B_{h/4}(y_i) \cap \Sigma$, and $\nu_{i+1}(0) = \nu_i(1)$. Set $\nu = \cup_{i=1}^n \nu_i$. □

This produces curves which are "h-almost monotone" in the sense that if $y \in \nu$, then $B_{4\,h}(y) \cap \nu$ has only one component which intersects $B_{2\,h}(y)$.

COROLLARY A.11. *If* $\Sigma \subset \{|x_3| \leq 2\,\beta_A\,h\}$ *and* E *is an unbounded component of*

$$\mathbf{R}^2 \setminus T_{h/4}(\Pi(\partial\Sigma))\,,$$

then $\Pi(\Sigma) \cap E = \emptyset$.

Proof. Given $y \in E$, choose a curve

$$\gamma : [0,1] \to \mathbf{R}^2 \setminus T_{h/4}(\Pi(\partial\Sigma))$$

with $|\gamma(0)| > \sup_{x\in\Sigma} |x| + h$ and $\gamma(1) = y$. Set

$$\Sigma_t = \{x \in \Sigma \,|\, f_{\gamma(t)}(x) = 3\,h/16\}\,.$$

By (A.6), we have $\Sigma_t \subset B_{7\,h/32}(\gamma(t))$, so that $\Sigma_0 = \emptyset$ and $\Sigma_t \cap \partial\Sigma = \emptyset$. By Lemma A.8, either:

- $\Sigma_t = \emptyset$, or
- Σ_t contains an arc of transverse intersection.

In particular, there cannot be a first $t > 0$ with $\Sigma_t \neq \emptyset$, which gives the corollary. □

COURANT INSTITUTE OF MATHEMATICAL SCIENCES, NEW YORK, NY and
MIT, CAMBRIDGE, MA
E-mail address: colding@cims.nyu.edu

JOHNS HOPKINS UNIVERSITY, BALTIMORE, MD
E-mail address: minicozz@math.jhu.edu

References

[ChY] S.Y. Cheng and S.-T. Yau, Differential equations on Riemannian manifolds and their geometric applications, *Comm. Pure Appl. Math.* **28** (1975), 333–354.

[CiSc] H. I. Choi and R. Schoen, The space of minimal embeddings of a surface into a three-dimensional manifold of positive Ricci curvature, *Invent. Math.* **81** (1985), 387–394.

[CM1] T. H. Colding and W. P. Minicozzi II, *Minimal Surfaces*, *Courant Lecture Notes in Mathematics* **4**, New York University Press, Courant Institute of Math. Sciences, New York (1999).

[CM2] ———, Estimates for parametric elliptic integrands, *Internat. Math. Res. Not.* **6** (2002), 291–297.

[CM3] ———, Minimal annuli with and without slits, *J. Symplectic Geom.* **1** (2001), 47–61.

[CM4] ———, The space of embedded minimal surfaces of fixed genus in a 3-manifold II; Multi-valued graphs in disks, *Ann. of Math.* **160** (2004), 69–92; math.AP/0210086.

[CM5] ———, The space of embedded minimal surfaces of fixed genus in a 3-manifold III; Planar domains, *Ann. of Math.*, to appear; math.AP/0210141.

[CM6] ———, The space of embedded minimal surfaces of fixed genus in a 3-manifold IV; Locally simply connected, *Ann. of Math.*, to appear; math.AP/0210119.

[CM7] ———, The space of embedded minimal surfaces of fixed genus in a 3-manifold V; Fixed genus, in preparation.

[CM8] ———, Embedded minimal disks, in *Minimal surfaces* (*MSRI*, 2001), *Clay Mathematics Proceedings*, 405–438, D. Hoffman, ed., AMS, Providence, RI, 2004.

[CM9] ———, Disks that are double spiral staircases, *Notices Amer. Math. Soc.* **50**, March (2003), 327–339.

[HoMe] D. Hoffman and W. Meeks III, The asymptotic behavior of properly embedded minimal surfaces of finite topology, *J. Amer. Math. Soc.* **2** (1989), 667–682.

[MeYa] W. Meeks III and S.-T. Yau, The existence of embedded minimal surfaces and the problem of uniqueness, *Math. Z.* **179** (1982), 151–168.

[Sc] R. Schoen, Estimates for stable minimal surfaces in three-dimensional manifolds, in *Seminar on Minimal Submanifolds*, *Ann. of Math. Studies*, **103**, 111–126, Princeton Univ. Press, Princeton, NJ (1983).

(Received June 30, 2001)